AD-A140 435 MATERIALS RESEARCH FOR ADVANCED INERTIAL INSTRUMENTATION TASK 2 GAS BEARI... (U) CHARLES STARK DRAPER LAB INC CAMBRIDGE MA K KUMAR ET AL. FEB 84 1/1

UNCLASSIFIED CSDL-R-1694 N00014-77-C-0388 F/G 17/7 NL

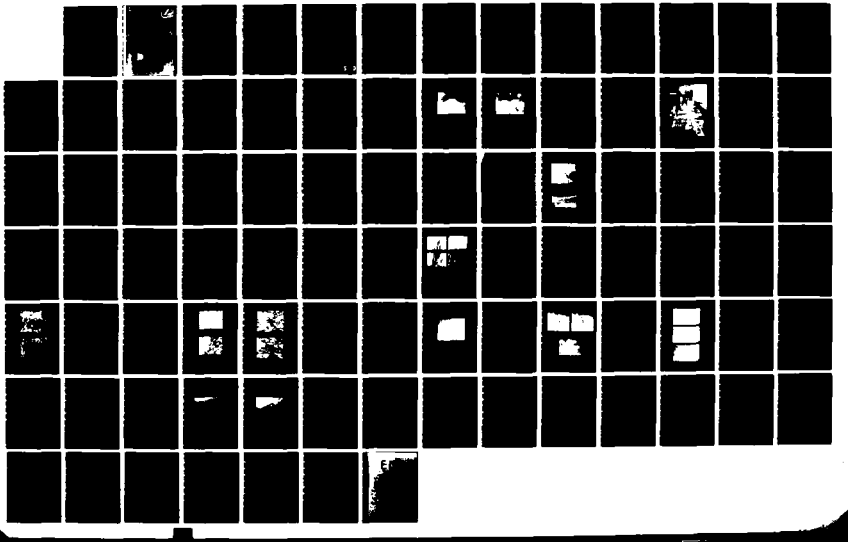

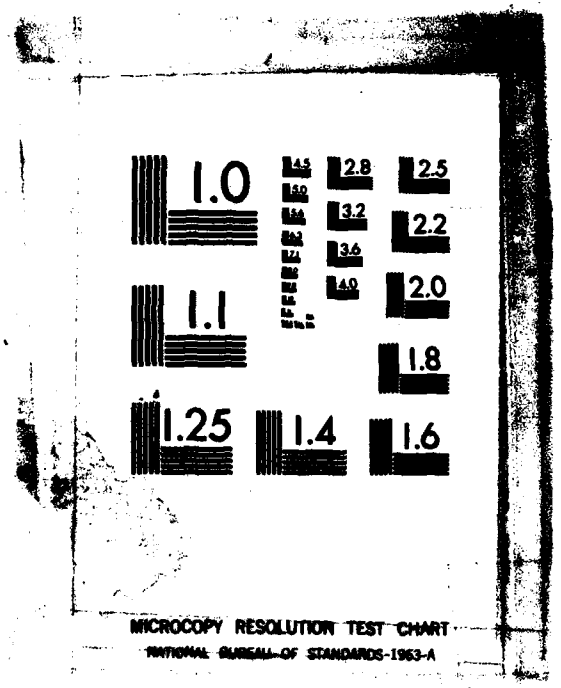
1.0
1.1
1.25
1.4
1.6
2.8
2.5
3.2
2.2
3.6
2.0
4.0
1.8
MICROCOPY RESOLUTION TEST CHART
NATIONAL BUREAU OF STANDARDS-1963-A

CSDL-R-1694

MATERIALS RESEARCH FOR ADVANCED INERTIAL INSTRUMENTATION

TASK 2: GAS BEARING MATERIAL DEVELOPMENT

FEBRUARY 1984

FINAL REPORT

BY

K. KUMAR, H. NEWBORN, D. DAS

Prepared for the Office of Naval Research, Department of the Navy
under Contract N00014-77-C-0388

The Charles Stark Draper Laboratory, Inc.
Cambridge, Massachusetts 02139

UNCLASSIFIED
SECURITY CLASSIFICATION OF THIS PAGE (When Data Entered)

REPORT DOCUMENTATION PAGE

READ INSTRUCTIONS BEFORE COMPLETING FORM

1. REPORT NUMBER: CSDL-R-1694	2. GOVT ACCESSION NO.: A140 435
3. RECIPIENT'S CATALOG NUMBER:	
4. TITLE (and Subtitle): MATERIALS RESEARCH FOR ADVANCED INERTIAL INSTRUMENTATION; TASK 2: GAS BEARING MATERIAL DEVELOPMENT	5. TYPE OF REPORT & PERIOD COVERED: Final Report 10/1/77 - 12/31/83
	6. PERFORMING ORG. REPORT NUMBER:
7. AUTHOR(s): K. Kumar, H. Newborn, D. Das	8. CONTRACT OR GRANT NUMBER(s): N00014-77-C-0388
9. PERFORMING ORGANIZATION NAME AND ADDRESS: The Charles Stark Draper Laboratory, Inc. 555 Technology Square Cambridge, MA 02139	10. PROGRAM ELEMENT, PROJECT, TASK AREA & WORK UNIT NUMBERS:
11. CONTROLLING OFFICE NAME AND ADDRESS: Office of Naval Research Department of the Navy 800 N. Quincy St., Arlington, Virginia 20217	12. REPORT DATE: February 1984
	13. NUMBER OF PAGES: 92
14. MONITORING AGENCY NAME & ADDRESS (If different from Controlling Office):	15. SECURITY CLASS. (of this report): Unclassified
	15a. DECLASSIFICATION/DOWNGRADING SCHEDULE:

16. DISTRIBUTION STATEMENT (of this Report)

Approved for public release; distribution unlimited.

17. DISTRIBUTION STATEMENT (of the abstract entered in Block 20, if different from Report)

18. SUPPLEMENTARY NOTES

19. KEY WORDS (Continue on reverse side if necessary and identify by block number)

Beryllium
Ion Implantation
CVD
Boron
Reactive Diffusion
Metal Matrix Composite
Beryllium-Ceramic Composite
Hot Isostatic Pressing (HIP)

20. ABSTRACT (Continue on reverse side if necessary and identify by block number)

The gas bearing materials research program was pursued with the aim of producing novel materials, with new technologies, for applicability to advanced inertial instrument designs. The objective was to produce low friction, high wear-resistance, high integrity gas bearing surfaces that were integrated within a beryllium structure. It was required that these surfaces not be limited in performance by factors known to influence

(OVER)

DD FORM 1 JAN 73 1473 EDITION OF 1 NOV 65 IS OBSOLETE

UNCLASSIFIED
SECURITY CLASSIFICATION OF THIS PAGE (When Data Entered)

existing hardware, such as porosity, adhesion, and nonconformity in physical properties to the several structural components.

Three approaches were selected to achieve the desired gas bearing surface. These included investigating reactive-diffusion bonded CVD-boron films on beryllium, boron-ion implanted beryllium surfaces, and Be-TiB_2 metal matrix composites. CVD-boron deposition on beryllium was found to proceed well in a high vacuum, bakeable, all stainless chamber. The successful procedure involved thermal decomposition of diborane on a beryllium sample surface which was heated by RF induction to about 700 to 800°C. Boron-ion implantation was performed on specially prepared beryllium surfaces, using a high current machine, up to boron concentrations of well over 50 atom percent. The Be-TiB_2 composites were produced by hot isostatic pressing (HIP) of blended and cold compacted beryllium and titanium diboride powders.

The surfaces produced with each of these technologies were investigated for friction and wear behavior. The CVD and implanted surfaces were additionally evaluated for structure (both micro- and crystal) as well as chemical composition (at the surface and as a function of depth). Techniques including optical microscopy, x-ray diffraction, electron microscopy, Rutherford Back Scattering (RBS), and Auger Electron Spectroscopy (AES) were employed for these examinations. A substantial level of effort was placed on developing appropriate lapping procedures as well as fabricating near-net-shape gas bearing parts with the Be-TiB_2 composites. Work in each of these areas resulted in surfaces that withstood wear and showed low values of friction coefficient, versus a diamond stylus. The surfaces of the implanted and the composite samples were found to be quite compatible, in a gas bearing wear circumstance, with several candidate mating materials as well. Even though the CVD-surfaces showed remarkably high values of microhardness (typically, well over 2000 KHN), these fared poorly against surfaces other than diamond. This led to decreased emphasis of this technology in the (later) hardware applicability and evaluation phase of this activity.

Several scientifically noteworthy accomplishments were achieved during this activity. Many of these were reported in the form of a large number of technical contributions to the open literature. More significantly, the initial objective of this activity (that of producing low friction, high wear resistance surfaces, integrated within a beryllium structure) was met. Experiments performed to study hardware applicability (of the different technologies pursued) showed that the ion implantation and Be-TiB_2 composite technologies were indeed capable of producing parts suitable to application (and without limitations from factors that influence performance in existing hardware). Additional work would be required to fully utilize surfaces produced using the CVD technique, principally as it relates to their wear and friction compatibility with candidate mating materials in gas bearings.

CSDL-R-1694

MATERIALS RESEARCH FOR ADVANCED INERTIAL INSTRUMENTATION

TASK 2: GAS BEARING MATERIAL DEVELOPMENT

FEBRUARY 1984

FINAL REPORT

by

K. Kumar, H. Newborn, D. Das

Prepared for the Office of Naval Research,
Department of the Navy, under Contract N00014-77-C-0388.

Approved:

M. S. Sapuppo, Head
Instrument Development Department

The Charles Stark Draper Laboratory, Inc.
Cambridge, Massachusetts 02139

ACKNOWLEDGEMENT

This report was prepared by The Charles Stark Draper Laboratory, Inc. under Contract N00014-77-C-0388 with the Office of Naval Research of the Department of the Navy. Ion implantation of the beryllium specimens and their Rutherford Back Scattering (RBS) evaluation was performed at the Naval Research Laboratory, Washington DC, under the direction of Dr. R. Kant.

Publication of this report does not constitute approval by the US Navy of the findings or conclusions contained herein. It is published for the exchange and stimulation of ideas.

TABLE OF CONTENTS

LIST OF FIGURES

LIST OF TABLES

SECTION 1

INTRODUCTION

The purely structural requirements of advanced inertial instruments (with respect to strength, stiffness, and creep) are adequately met through the use of instrument-grade beryllium. The mating surfaces of the gas bearings of these instruments, however, require higher hardness and greater wear resistance than beryllium offers. A variety of combinations of materials and processes consisting of solid ceramics and arc-plasma sprayed or sputter-deposited ceramics on beryllium surfaces have been used. None of these is completely satisfactory because of considerations such as thermal expansion and conductivity mismatch, poor adhesion, and existence of porosity.

Initial work performed at The Charles Stark Draper Laboratory, Inc. (CSDL) and at other laboratories involved fabricating entire bearings out of solid pieces of ceramic.[1]* These ceramics were typically produced by sintering and hot pressing techniques. Difficulties were encountered in machining these materials, making the process expensive and time consuming. An additional disadvantage in the use of ceramics for this purpose was the physical incompatibility of the resultant gas bearings with the other structural members of the gyro. (Differences in thermal expansion characteristics and low values of thermal conductivity of these materials result in undesirable strains and temperature variations in the assembly. This leads to a variety of instrument instabilities that adversely affect the accuracy and reliability of the several inertial components.) The high cost in money and time, in addition to the problems stemming from low values of

* Superscript numerals refer to similarly numbered items in the List of References.

thermal expansion and thermal conductivity for ceramics, caused this option to be discarded.

The subsequent rationale developed to resolve the discrepancies associated with the use of monolithic ceramics envisioned the use of two different materials, since no single material was known to meet all demands. One material (beryllium) was to form the structural member and satisfy bulk property requirements. The other was to be deposited as a coating to yield a low-friction, wear-resistant surface for the gas bearing. Nevertheless, operational and processing problems persisted even with the approaches that resulted from this rationale, and the need for a better materials system has continued. The present task has addressed this latter requirement through research efforts on new materials and processes for gyroscope gas bearings. Much of the work performed in this program was reported on an interim, annual basis, and is described in detail in References 2 through 6. Several of the highlights, however, have been included in this final report.

SECTION 2

MATERIALS PROPERTY REQUIREMENTS

2.1 Bulk Properties

Since the basic structure of the instruments consists largely of beryllium, this material is also the best choice for the structures supporting the gas bearing surfaces. The bulk property requirements which it meets are:

(1) High strength-to-density ratio (important from design considerations)

(2) High thermal conductivity (to avoid temperature gradients)

(3) Nonmagnetic (to eliminate interference with electromagnetic circuitry)

(4) Thermal expansion compatibility with other structural members

(5) Finishable to accurate tolerances of better than 1 microinch

2.2 Coating Properties

Ideally, the material to be applied to the gas bearing surface as a coating would be very similar in its own bulk properties to those of the underlying structure. For that reason, the above listing also applies to the coating material, although less critically so where thinner coatings are considered. On the other hand, considerably greater importance must be attached to the surface properties, the most significant of which are:

(1) High resistance to wear from sliding, erosion, and impact, for extended bearing life and stable performance

(2) Low coefficient of friction for minimum starting torque

(3) Zero surface porosity, for maximum gas bearing stiffness and minimum contamination entrapment

2.3 Coating Technology

Materials that are hard enough to be of interest as wear-resistant coatings generally have such high melting temperatures as to require special methods of application. Two methods that have received attention in this area are plasma-spraying and sputtering.[7,8] With plasma spraying it is easy to apply coatings that are several thousandths of an inch thick, while the thicknesses of sputtered films are generally less than that by about two orders of magnitude. Examples of the use of these processes are the plasma-sprayed chromium oxide and the sputter-deposited tungsten carbide and titanium carbide coatings that have been subjects of past development activity.

2.4 Limitations of Present Technology

The one feature common to both sprayed and sputtered coatings is the difference in physical properties between the coating and the substrate. While this may be somewhat tolerable in thin films produced by sputtering, thicker films made by spraying are susceptible to failure from imperfect match of expansion coefficients at the coating-substrate interface. To reduce stresses that result from differences in expansion coefficients, spraying is generally conducted at lower spray temperatures. However, this adversely affects interparticle cohesive strength, which results in pull-outs during polishing and lapping operations and generation of wear debris in active service. The clearance between the mating parts of a gas bearing is only about 50 microinches, so that even the mildest form of wear (mildest by

conventional standards) can prove to be catastrophic in gas bearing applications.

A more severe problem that has been found in sprayed deposits is the presence of interconnecting porous structures in the coating. The effect of this interconnected porosity is to provide a shunt path for gas flow such that the hydrodynamic pressure rise is attenuated from that attainable with a nonporous coating. This, in turn, causes a lower load capacity and stiffness for the gas bearing. In addition to this most severe effect, the porosity at the surface also results in effectively increasing the bearing gap beyond the physical (design) clearance. Although machining problems in sprayed deposits are less than those for sintered products (because parts are sprayed close to final size), they are present albeit to a lesser degree on a small scale.

The adhesion of the coating to the substrate is an important consideration in wear performance. The forces that give rise to adhesion in films made from both these processes can be both mechanical and chemical in nature. The adhesion observed for deposits fabricated using the arc-plasma technology is generally found to be influenced by mechanical interlocking of the film on the external features of a substrate. However, in both cases, chemical forces frequently give rise to stronger interfacial bonds. This type of bond is often termed a metallurgical or a diffusion bond. In chemically compatible coating-substrate systems, the adhesion strength can be increased by depositing films at elevated temperatures [as in chemical vapor deposition (CVD) or in physical deposition by sputtering or spraying] or by subjecting the substrate-coating composite to high temperatures after deposition. The former approach can result in a compressive state of the ceramic deposit at operating temperatures, whereas the latter may produce cracking in the deposit because of the tensile nature of the stress that will act on the ceramic coating upon heating. Elevated temperature deposition is therefore preferable to post-deposition heat treatment since ceramic materials generally behave well under a mild compressive loading.

Poor adhesion has been a severe problem with sputtered ceramic coatings formed on beryllium substrates.[9] Sputtered films have also shown large deviations from stoichiometric composition and the presence of undesirable microstructures. Depending on the conditions employed during fabrication, the structure of sputtered films could be either amorphous or crystalline. Columnar growth structures with poor interparticle bonding are frequently encountered in sputter deposits.

The various types of materials and process options, as discussed above, which have been investigated at CSDL and other similar laboratories are shown in Table 1. Also listed are the options that were investigated during the performance of the work describe in this report.

Table 1. Materials and process options considered for bearing fabrication.

Material	Process	Problems Encountered
Solid Ceramic	Sintering and Hot Pressing	Difficult to Machine Physical Incompatibility Low Thermal Expansion Poor Thermal Conductivity
Hard Coatings	Plasma Spraying (Thick)	Porosity, Adhesion, Cohesion, Plus Above
	Sputtering (Thin)	Adhesion, Composition, Structure Mismatch Less Critical Because of Coating Thinness
Modified Surface	Case Hardening by Alloying of the Surface	None Perceived
Composite	Powder Metallurgy-Hot Isostatic Pressing	None Perceived

2.5 Direction of the Present Work

The broad objective which underlies all aspects of the present effort is to establish a hard, pore-free, wear-resistant surface which is integral with the beryllium structural members, thus eliminating the adhesion problems that have been encountered in the past. In the case-hardening subtasks this is approached by treating the beryllium surface with a material (boron) with which it forms hard compounds. Boron enrichment of the surface, in one process, is accomplished by reactive diffusion of a freshly formed film of boron with the underlying beryllium. In another part of the work, boron ions are forced by an electrical potential to penetrate into the beryllium surface by ion implantation, a process which is relatively immune to native oxide barriers, solid solubilities, and diffusion coefficients.

In another subtask the desired hardening and wear resistance are imparted by particles of a hard ceramic phase dispersed within the beryllium matrix. Such a metal-matrix composite has been produced using powder metallurgy methods.

SECTION 3

BERYLLIUM-BORON REACTIVE DIFFUSION BY CVD

3.1 Introduction

After much experimentation, adherent boron-rich coatings can now be reproducibly deposited on beryllium substrates by the chemical vapor deposition process. Although measurements have indicated significant improvements in surface hardness (1400 to 1800 KHN for the coatings, versus 400 to 600 KHN for beryllium), friction and wear data using the pin-on-disk method have consistently shown high friction values and more than acceptable levels of wear at low applied loads when materials other than diamonds were used for the pin. Pin-on-disk tests were conducted to include matching of the CVD disk surface with a variety of pin materials including diamond, sapphire, CVD B-Be, and a Be-TiB_2 composite. The high measured values of the friction coefficients and the observed destruction of the coatings with low pin loadings (for pin materials other than diamond) led to a decreased emphasis of this technology compared to the other alternatives developed under this program for making advanced gas bearing hardware.

3.2 Goal

The primary goal of this subtask of the gas bearing materials program was to produce a hard, wear-resistant, low-friction surface on beryllium by reactive diffusion of beryllium with boron. A secondary objective of this program was to study the relevant diffusion kinetics in the Be-B system in order to be able to exercise control on the structural and compositional characteristics of the coating.

The binary alloy system Be-B contains a number of intermetallic compounds, of which the compounds BeB_6 and BeB_2 are reported to have hardness values of 2600 and 3200 KHN, respectively.[10,11] Boron also

has a hardness value of nearly 3000 KHN. Therefore, reactive diffusion of boron provided an attractive means of producing metallurgically bonded hard coatings on the beryllium surface.

3.3 Results and Discussions

Work performed in this subtask was primarily concentrated on: (1) attempting to obtain relevant information on Be-B diffusion kinetics, (2) achieving successful chemical vapor deposition of boron coatings on beryllium, and (3) characterizing the CVD coatings for their chemical and tribological behavior. The aim of this study was to examine the potential applicability of reactively bonded Be-boride compounds (produced on beryllium surfaces) to gas bearing hardware fabrication. Work performed in each of these areas is described below.

3.3.1 Diffusivity Studies

Early in the program, attempts were made to perform diffusion studies to determine optimal heat treatments for the bonding of boron to beryllium and for the formation of the hard Be-B phases. Investigations aimed at determining diffusion kinetics in this system required metallurgically bonded beryllium and boron diffusion couples. Difficulties were encountered in attempts to form diffusion couples with beryllium and boron discs even when they were subjected to high pressure at up to 1000°C. There was no resulting bonding or evidence of a significant reaction in these experiments. Likewise, boron slurry-coated beryllium samples produced no bonding between beryllium and boron at temperatures of up to 1000°C. Sputter-deposited boron coatings (0.5 and 1.0 micron thick) on beryllium surfaces gave partially adherent layers, which were subsequently heat treated. Heavier boron deposits (3.0 microns thick) formed using ion plating produced nonadherent coatings which, as a result, could not be heat treated. It was suspected that the observed nonadherence might have resulted from one or more of the following:

(1) The structural type of boron used for the experiments [12-14] (different boron types include a high-temperature β-form, a low-temperature γ-form, and amorphous boron)

(2) A barrier layer of beryllium oxide, which may have prevented the formation of the diffusion bond, and

(3) Thermal expansion incompatibility between beryllium and the borides that were formed, that may have led to separation upon cooling from high temperature

Efforts were subsequently directed toward eliminating the oxide which Auger analysis showed existed as heavy BeO layers at the surface. Solid beryllium and amorphous boron powder were pressed together in a unique hot-pressing technique[15] (in an attempt to form a Be-B diffusion couple) at 1000°C for 24 hours in an ultraclean, high-vacuum environment. The reacted sample consisted of the following successive layers: Be, BeO, BeB_2, BeB_6, and B. The oxide layer on beryllium was again quite substantial. It was felt that the boron powder was the source of the observed oxygen. On the boron side of the oxide layer, there were two distinct measurable layers of beryllium borides. The first was a comparatively thin metallic gray layer and the other a thick brick-red color layer. X-ray diffraction was used to identify the two layers as BeB_2 and BeB_6, respectively. It was noted that these high-boron beryllium-boride compounds could be formed using amorphous boron at temperatures as low as 1000°C. The reacted sample, however, came apart at the interface between the layers BeO and BeB_2.

A second approach to produce diffusion couples between beryllium and boron succeeded in producing a well-bonded couple with no intervening BeO layer. A β-boron rod was buried in high-purity beryllium powder. The powder was cold isostatically pressed and then hot isostatically pressed around the boron sample. Hot isostatic pressing (HIP) was carried out in an evacuated and sealed iron container which was thoroughly outgassed prior to HIP. The HIP operation was

performed under an argon gas pressure of 15 kpsi and a temperature of 950°C for a period of two hours. The diffusion couple thus formed was removed from the container, and metallographically polished to reveal a bonded interface with a diffusion zone about 10 microns thick. It appeared that four layers existed within this zone. Since the structural form of boron that was expected to be formed as a result of the techniques under investigation was the low-temperature γ-form, it was considered desirable to perform diffusion kinetics studies with both the β and γ forms of boron. β-boron was commercially available; however, γ-boron, the phase most likely to be present at the deposition temperatures, was not. γ-boron pieces were fabricated at CSDL by use of an arc plasma spray technique which was investigated for this purpose.[16,17] Subsequently, as with the β-boron rod sample, Be-γB couples were successfully fabricated by the HIP technique. In the diffusion couples formed with both β- as well as γ-boron, good diffusion interfaces were formed between beryllium and boron in the as-HIP condition. The as-HIP interface observed between beryllium and γB is shown in Figure 1. The dark areas within the interface were believed to be pull-outs from polishing and, therefore, not considered detrimental to performing post-HIP diffusion heat treatments. However, when post-HIP diffusion heat treatments were performed with these couples at elevated temperatures, unexpected failures resulted. Metallographic examination of the interfaces showed that the beryllium had separated from the diffusion zone. This separation must have occurred at a very early stage of the diffusion heat treatment, since there was no apparent growth of the diffusion zone. An area of the heat treated interface in the Be-γB diffusion couple is shown in Figure 2.

In spite of failure at generating relevant diffusion data through the use of conventional diffusion couples, another possibility of obtaining useful information was expected to come from heat treatment of CVD processed samples. Chemical vapor deposition of boron on beryllium was performed using diborane gas. These studies are described in more detail in the next section. X-ray analysis showed that an amorphous boron layer on beryllium converted to the compound BeB_6 upon subjecting

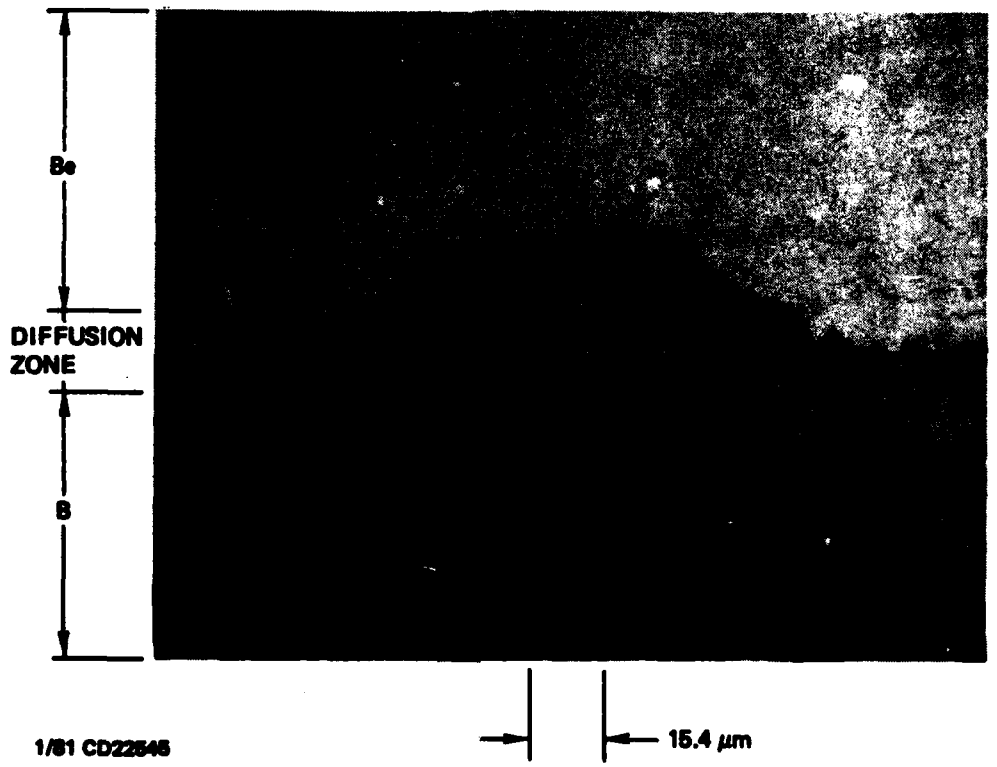

Figure 1. Polished as-HIP interface of Be-γB diffusion couple formed by HIPing γB pieces surrounded by Be powder.

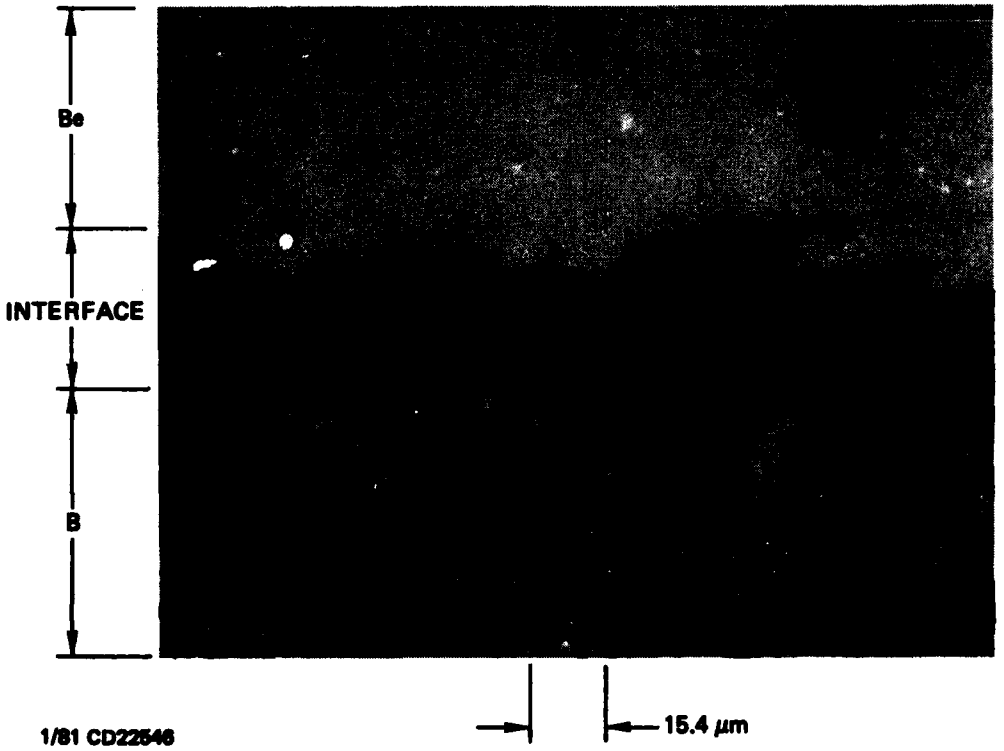

Figure 2. The interface between Be and B shows that Be has pulled away during the attempted diffusion heat treatment at 900°C.

the coated surface to a post-deposition heat treatment. Heat treatment of CVD samples at temperatures ranging from 750°C to 900°C showed that at the lower heat treatment temperatures there was little change in coating appearance.

At the higher temperatures, however, peeling off of the coating was prominent. Again, the experiments yielded limited quantitative data as to the the diffusion kinetics in the Be-B system.

3.3.2 Chemical Vapor Deposition: Processing

Initial CVD experiments were performed in a simple system which was built quickly and inexpensively. A 1.25-inch-diameter quartz tube capable of being evacuated to 10-millitorr pressure constituted the CVD chamber. The beryllium sample was located inside the tube and heated to the desired temperature by means of an RF induction coil placed around the tube. The CVD gas was then allowed to flow through the tube at the desired flow rates.

The CVD gas systems investigated included: (1) reaction of boron trichloride (BCl_3) with hydrogen, and (2) thermal decomposition of diborane (B_2H_6). The depositions were carried out at temperatures in the range of 900°C to 1000°C. The coatings were on the order of a micrometer in thickness, and showed hardness values of approximately 1200 KHN. The color of the coatings (rusty pink) and Auger electron spectroscopy indicated the occurrence of chemical reaction between beryllium and boron, with the formation of compounds belonging to the Be-B system. Although no positive identification of the compounds was made, it was suspected that the compounds were beryllium-rich (based both on Auger analysis and on the rather low values of hardness that were measured). Thicker coatings were attempted, but coatings thicker than about 1 micrometer tended to crack and spall. Experiments showed that thermal decomposition of diborane was the preferred procedure for forming boron films on the beryllium surface.[18] Up to 5-micron-thick,

steel-gray coatings were subsequently formed at temperatures of 700 to 800°C. Microhardness values on the order of 2000 KHN were measured for these latter coatings. The capability to make even thicker, hard coatings at low deposition temperatures was realized after the construction of an improved CVD system.

The new CVD system that was built (Figure 3) consisted of a stainless steel bell jar equipped with high vacuum pumping systems and all stainless steel plumbing. The system was capable of being baked out and achieving a high vacuum of about 10^{-7} torr. A 20-kw RF generator was acquired for furnishing induction heating power to the coil located inside the bell jar. The larger size of the new coil permitted increasing the sample size from 1/2-inch-diameter discs to larger sample sizes. The new capability was consequently determined to be adequate for producing CVD coatings on actual gas bearing components (should that be deemed desirable).

Initial experiments in this new system were performed on 1/2-inch-diameter samples using a 3/4-inch-inner-diameter (ID) RF coil. The CVD procedure involved evacuating and baking-out of the system at a low temperature of 100°C, following which the CVD was carried out using thermal decomposition of argon-diluted diborane gas (99.9% A + 0.1% B_2H_6) at atmospheric pressure. During the CVD run, the bell jar was water-cooled to prevent evolution of undesirable gases from the CVD chamber walls. Well-bonded coatings of up to 10-μm thickness, with uniform coverage over the entire 1/2-inch-diameter surface, were obtained at 700 and 800°C. Measured microhardness values exceeded 3000 KHN under a 25-gram indentation load. (The low-temperature CVD samples prepared in the older CVD apparatus had hardness values of around 1000 KHN at a 25-gram load although at a 5- to 10-gram load the measured values were above 2000 KHN.) Therefore, the quality of the coatings was found to have improved measurably.[18] Metallography, electron diffraction, and Auger analysis of these latest samples suggested that the CVD coatings consisted of an amorphous outer layer of boron with a series of boride compounds sandwiched between the outer boron layer and the beryllium substrate.

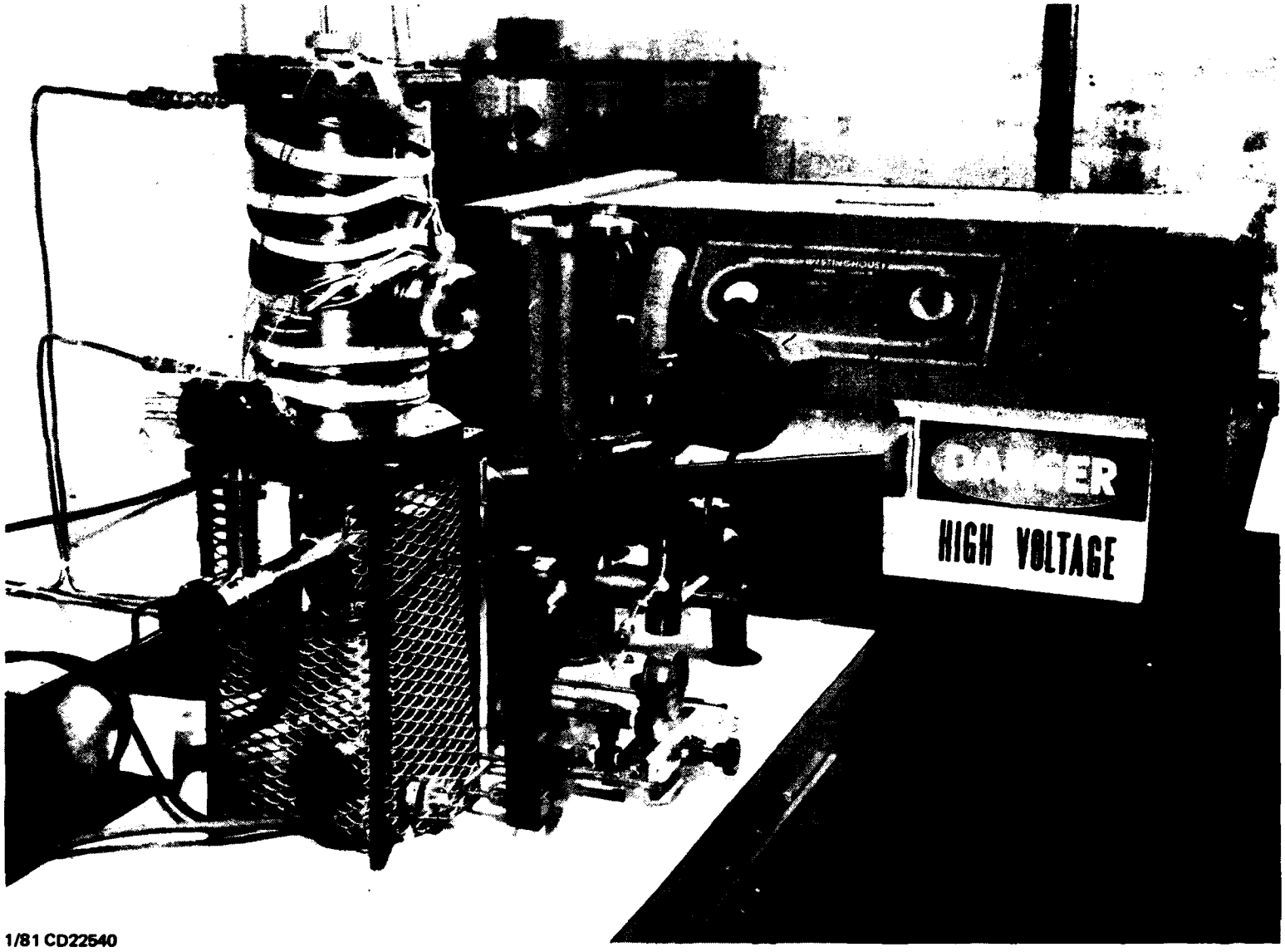

1/81 CD22540
TSA 3958

Figure 3. An overall view of the new CVD system. Stainless steel bell jar with necessary plumbings is located on table top. The 25 KW RF generator is located to the right of the table.

Subsequently, the disc sample size was increased to 3/4 inch diameter. (This larger size facilitated the evaluation of these coatings for friction and wear behavior.) Problems related to thickness non-uniformity and non-reproducibility of reactant gas compositions were encountered in work with the 3/4-inch-diameter samples. The first problem was resolved through sample rotation; the second through controlled and systematic dilution of the diborane gas (with added argon) during deposition.[19] The best coating condition was achieved with a very low diborane concentration at the lowest temperature that was attempted, 725°C. The low diborane concentration levels that were used successfully resulted from mixing the diborane gas mixture with argon at flow rates of 45 cm^3/min (and less) and 800 cm^3/min, respectively. Run conditions for the several CVD-coated disks are summarized in Table 2. A second series of runs identified as samples 92 through 95 and 101 in Table 2 was subsequently performed in order to demonstrate the reproducibility of the resultant coatings. The results were found to be quite reproducible with respect to visual appearance and tribological behavior.

3.3.3 Chemical Vapor Deposition: Analysis

3.3.3.1 Auger Spectroscopy

Auger electron spectroscopy was determined to be capable of providing accurate information with respect to chemical analysis of thin films composed of the compounds of boron and beryllium. The analytical procedure consisted of continuous removal of material away from the coated surface by sputtering it with argon ions. While the material was being removed, the chemical composition of the exposed surface was simultaneously determined. The composition data thus obtained from the several samples were plotted against sputtering time. The total depth to which the composition evaluation was performed, as a result of the sputtering, was independently determined using a Dektak surface profilometer. The measured value of the sputtering rate calibrated in this manner was found to be about 0.04 μm/minute. (The sputtering time,

Table 2. Quality of the CVD coating as a function of temperature, deposition time, and gas composition.

Sample No.	Substrate Temp, °C	Deposition Time (hrs)	Gas Flow rate, cm^3/min		Coating Quality Remarks
			B_2H_6+A	A	
65,94, 95	725	3	36	800	Adherent, metallic gray, shiny
66	725	2	72	800	Nonadherent, sooty
67	725	3	36	800	Repeat of No. 65. Results same as No. 65.
68,93	725	3	54	800	Hard, adherent, gray
69,92	725	3	45	800	Shiny gray
70	725	1.5	63	800	Pink, adherent
71	725	1.7	63	800	3 additional hours at room temp. in argon. Shiny, gold.
72,101	825	2	72	800	Adherent, shiny blue
73	825	1	72	800	Adherent, shiny silvery
74	825	0.5	72	800	Adherent, shiny blue-gray
75	825	4	72	800	Dull gray, adherent

therefore, could be converted to depth in μm by multiplying the number of minutes on the depth profile plots by 0.04.)

Many of the coatings that adhered well to the surface were found to be greater than 10 μm in thickness. It was observed that the higher the diborane content, the more likely was the incidence of the coating appearing sooty. It was noted that a wide range of Be/B ratios appeared in the coatings and these were a strong function of the diborane concentration. For the lowest gas concentration, pure boron was found to form reproducibly (sample Nos. 65, 67). Similar observations with respect to possible phases with increasing depth from the surface were observed for samples 69, 72, 73, and 74, while No. 68 contained, in the main, a 2 to 1 ratio of Be/B at the surface. (Samples 69, 71, 72, 73, and 74 also had this phase, deeper into the sample, but in limited quantity.) No attempts were made to identify the phase compositions from the chemical analyses that were performed; however, some of the chemical compositions that were observed appeared not to correlate to the known intermediate phases between beryllium and boron.

Wear testing was performed on the many above samples prior to their evaluation with Auger electron spectroscopy. In order to provide a smooth surface for wear testing, an approximately 2-μm sample of the film was removed in each instance by a gentle polishing procedure. Therefore, the depth profile of each sample was incomplete in that the characteristics of the top 2 μm of the surface were not represented. However, the chemical composition found at the beginning of the depth profile analysis was also the chemistry of the surface on which the wear and friction tests were performed and, therefore, considered relevant to this study.

3.3.3.2 Wear and Friction Tests

The testing mode selected for the CVD-coated samples was the pin-on-disc procedure. The pin consisted of either a rigidly held 1/8-inch-diameter ball or a solid cylindrical rod with an equivalent radius

formed at one end. The dead load applied on the stationary pin was 30 gm. It was located on the rotating sample about 0.25 inch away from the center of rotation. Samples were rotated at speeds of 200 r/min or 100 r/min for 5 to 10 minutes with the resulting circular wear tracks approximately 1/2 inch in diameter. The rotation of the test disc required a restraining torque on the pin to maintain its position. This restraining torque was a direct measure of the dynamic friction coefficient between the pin and the disc[20] and was given by

$$T = \mu PR$$

where

T is the torque
P is the normal load
R is the radius of the wear track
μ is the friction coefficient

The output E_o (in mV) from the signal generator was proportional to the torque:

$$E_o = S_{SG}T$$

where

S_{SG} was the signal generator sensitivity (calibrated at 134 mV/in-oz for the CSDL apparatus).

Therefore

$$\mu = \frac{E_o}{S_{SG}} \times \frac{1}{PR} \quad (P \text{ in 'oz,' } R \text{ in 'in'})$$

Slower speed (100 r/min), longer time (10 minutes) pin-on-disk tests on the polished, boron-coated beryllium samples consistently gave reproducible results. The measured value of the friction coefficient was always between 0.3 and 0.4 when the surface was tested against sapphire. In general, it was found that the higher the initial value of the friction coefficient (μ), the lower was the load at which substantial wear was observed. Wear results for samples 69 and 74 showed that use of a diamond pin, in contrast to use of the sapphire pin, provided for lower values of μ and a reduced level of wear during these tests. It should be noted that substantial (unacceptable) wear was evident even for a 20-gram loading with the sapphire pin. The surface performed considerably better versus the diamond pin.

Because the eventual end use of these coated materials would be in a gas bearing wheel assembly, it was considered pertinent to use potential matching hardware material(s) as the pin in subsequent wear tests. Attempts were also made to coat beryllium pin surfaces by CVD. (Several CVD-coated pins were made to examine the compatibility of the coated beryllium surface versus itself.) In all of the wear tests that involved the CVD pins, the coated pin surface was destroyed. Another candidate gas bearing material, the Be-TiB_2 composite developed under this program, and described later in the report, was fabricated into a rod, given the correct tip curvature at one end, and polished for use as a pin. Samples 92 through 95 and 101 were tested against both sapphire and Be-TiB_2. The tests against the composite were the most stringent, as friction coefficients generally were greater than 0.3 at a 20-gram loading. However, sample 93 (which was similar to No. 68) showed an anomalous μ value of only 0.17 at a 20-gram load with the composite. (Auger analysis of No. 68 had revealed a Be/B ratio on its surface which had suggested a more beryllium-rich phase at the surface than was observed for most of the other samples.) In the other samples, this phase appeared to exist in the subsurface layers at a finite depth from the surface. The low friction coefficient value for sample 93 led to a 30-gram loading test. Profilometer traces indicated that the depth of these grooves was on the order of 0.2 to 0.4 μm. This sample exhibited

a high degree of friction for the first few minutes of test (presumably, as the groove was being cut,) followed by steady-state wear with no evidence of catastrophic wear. (Severe wear is usually connoted by ragged tracks.) From the present testing procedure it could not be determined whether the coating was merely being compressed and/or whether the underlying beryllium was being deformed.

SECTION 4

ION IMPLANTATION

4.1 Introduction

The ion implantation effort was pursued jointly with the Naval Research Laboratory (NRL). Most of the implantations performed to date were done at NRL. The subsequent evaluation of the implanted surfaces was accomplished mostly at CSDL. The results of this effort have shown this to be both a viable, as well as, possibly desirable technology for producing gas bearing surfaces. The implantation technology was developed to the extent of producing experimental prototype hardware and performing evaluations to demonstrate its feasibility for application. The surfaces produced on beryllium through boron ion implantation proved to be substantially compatible with other candidate materials that could be used as mating materials in instrument gas bearings. The potential applicablity of this technology to advanced instrument design appears high from the results that were achieved during this program.

4.2 Goal

As in the CVD subtask, the objective of this effort was also to produce a hard, wear-resistant, low-friction surface on beryllium through modification of the surface composition and structure. Here, beryllium surface modification was produced through implantation of boron into beryllium. (The rationale for selecting boron as the implantation species derives from the extremely high levels of hardness that are associated with the high-boron containing Be-B compounds.)

4.2.1 Process Description

The ion implantation process differs from those based on diffusion by employing kinetic, rather than thermal, energy to introduce and emplace the foreign species which is intended to modify the host material. A high kinetic energy is given to the species to be implanted, such as boron, by first ionizing the boron atoms and then accelerating the ions through an electrical potential difference. They are then directed as a beam (or current) of ions onto a substrate material, such as beryllium, whose surface their high kinetic energy allows them to penetrate. The quantity or dose of boron delivered is determined by the magnitude of the current and the length of time for which it is applied. The range of penetration of the ions depends on the accelerating potential. Consequently, for ion implantation processing, the concentration of boron in the surface of the beryllium is not limited to its solid solubility, and the penetration of boron into the beryllium is not restricted either by the diffusivity of the boron or by the presence of a native oxide film on the beryllium. A principal feature of ion implantation is therefore the unique degree of control which it affords in generating alloyed surface layers.

4.3 Results and Discussions

Work performed in this subtask was essentially concentrated in three broad areas. These included: (1) performing experiments to implant boron into beryllium with specific depth composition profiles, (2) characterizing the implanted surfaces for microstructure, chemistry, and tribological behavior, and (3) producing and testing of hardware produced with the boron implantation technology. Work performed in each of these areas is described below.

4.3.1 Implantation Studies

The first few samples of beryllium implanted with boron were prepared at the Naval Research Laboratory in a low current machine so that the processing time requirement was inordinately long, but they sufficed to show that significant boron concentrations could be attained in beryllium surfaces. Two independent methods of assessing erosion due to sputtering indicated that it was negligible and, therefore, did not set any serious limits on the concentrations which might be reached. In this phase, the specimens prepared were calculated to contain 10, 20 and 40 atomic percent boron concentrations uniformly distributed within a layer 0.8 μm deep. Hardening, as tested with a Knoop indenter, ocurred upon implantation[21] and increased further with heat treatment; the hardness increase on heating was considered to be an indication that the initial hardening was a result of compound or quasi-compound formation and not primarily due to lattice strains stemming from the intrusion of a foreign species. This earlier interpretation appeared consistent with Rutherford back-scattering measurements done on some of these samples at the Naval Research Laboratory (NRL).

Subsequent work on a second group of specimens, which were each of a size large enough to permit friction and wear testing after implantation, was performed in a new implanter with a higher current capability. These samples were implanted to levels of 60 and 40 atom percent boron in beryllium and again showed hardness increases.[22] However, inconsistencies and a lack of frequent reproducibilty showed the need for better sample thermal control during implantation and examination of more than a single sample of a given type.

A variety of additional implants were performed. Included among these were flat, graded, and single dose concentration profiles. The ion implantation was conducted at a target chamber pressure of 10^{-6} Torr and the sample temperature was not allowed to exceed 160°C during implantation. The samples were firmly clamped to a water cooled holder and a thin sheet of indium was used to improve the thermal conduction at

the sample/holder interface. The samples were held at low temperature in order to retard oxidation of the beryllium and to minimize the mobility of the implanted boron.

Most of the experimental work was performed on beryllium samples fabricated with one of two types of implantation profiles. One of these was designed to produce a reasonably flat boron concentration profile from 0.1 μm to 0.65 μm beneath the surface. For the other, the doses were tailored to generate a graded boron concentration profile which peaked close to the surface and decreased gradually with increasing depth. Table 3 is a list of the doses and ion beam energies used to produce the flat and graded distributions. The values shown in Table 3 correspond, theoretically, to doses required to achieve flat and graded profile samples with peak concentration values of 10 atom percent. The fluences used for samples produced with intended compositions of 20, 30, and 40 atom percent boron were two, three, and four times, respectively, the values shown in Table 3. As stated earlier, the energy of the incident boron ions determined the depth of penetration of the ions into the beryllium surface (the higher the energy, the greater the depth) and the boron ion fluence (which is related to the current density at the substrate) determined the atomic concentration at a given depth.

Table 3. Boron doses (x 10^{16} B/cm^2) and implantation energies theoretically calculated to produce flat and graded profile samples of 10 atom percent boron peak concentration.

Sample	Energy (keV)					
Profile	25	43	67	100	140	192
Flat	7.1	9.6	10.2	13.2	14.2	15.2
Graded	7.1	8.6	8.8	8.0	6.3	3.8

4.3.2 Analytical Evaluations

4.3.2.1 Microstructure

4.3.2.1.1 Optical Microscopy

Figure 4 shows a typical Nomarski view towards the edge of an NRL-produced 40 atom percent boron implanted beryllium disc sample. In the process of holding the specimen firmly inside the holder during implantation, regions close to the edge of the disc were partly covered. This, therefore, resulted in boron implantation into most, but not all, of the sample surface.

The view in Figure 4(A) shows both the implanted and the unimplanted area. It was interesting to note the considerably increased level of detail in the microstructure (boundaries, twins) observed in the implanted regions compared to the unimplanted regions. This obviously indicated that although substantial removal of beryllium from the surface did not occur during boron implantation (as had been demonstrated),[21] the surface was nevertheless gradually etched away by the incident ion beam.

It was noted that whereas these effects were clearly visible when the sample was examined using the differential phase contrast (Nomarski) technique, these details were lost when the sample was examined using the more conventional procedure of polarized light microscopy (Figure 4B). The latter is the widely used technique for the optical examination of the microstructures of beryllium.

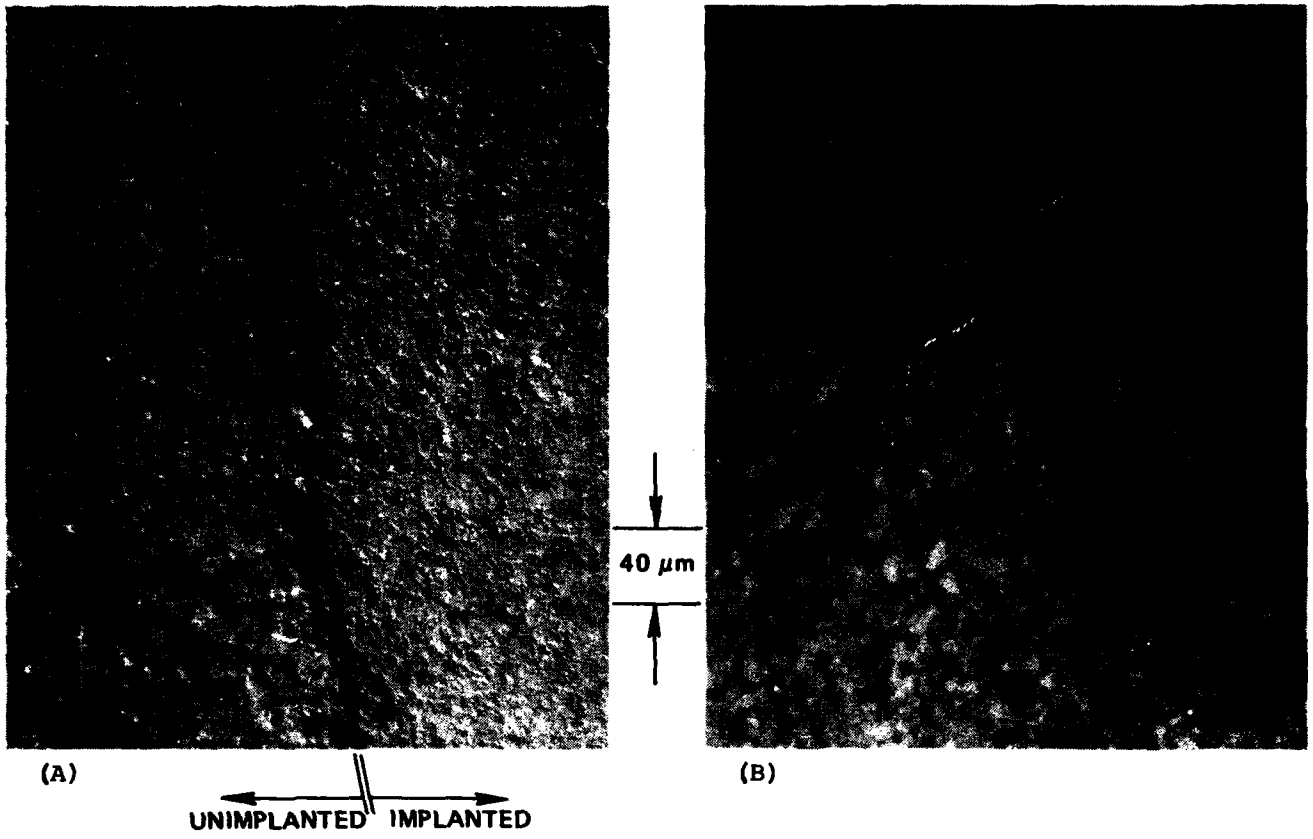

Figure 4. Micrographs showing (A) Etching of sample NRL 40-VI from the implantation process, Nomarski, and (B) polarized light micrograph of the same region showing grain structure.

4.3.2.1.2 Electron Microscopy

Microstructure evaluations of the implanted layers were initially attempted using reflection electron diffraction (RED) when it was realized that use of the transmission electron microscopy (TEM) and diffraction technique posed logistical problems. The results obtained by RED on implanted surfaces were inconclusive in that no clear diffraction pattern was obtained from the surface.

Subsequent RED examination of as-polished, unimplanted beryllium surfaces also showed the absence of a diffraction pattern; however, the existence of a well-defined beryllium pattern was clearly observed when the unimplanted beryllium sample was stress relieved for one hour at about 790°C. This suggested that the observed amorphous nature of the surface in the implanted specimens might well have resulted from the sample preparation procedure that was adopted prior to implantation of the specimens and may or may not be related to the implantation of the boron species. The importance of good surface finish, freedom from scratches, and superior flatness was also determined to be significant for determinations of microhardness indentation measurements and accurate surface profilometry, which was employed for studying wear effects from the tests that were performed.

Arrangements were made for a large group of discs to be cut from a give lot of beryllium and to be lapped and polished at an organization (Applied Optics Center Corporation) which is well established in the field of beryllium mirror polishing. This was only partially successful because only a few discs in the first shipment were acceptable. The difficulty was traced to the omission of a special stress relieving heat-treatment between sample machining and the lapping/polishing operation. This omission was corrected and the balance of the starting material was procured as adequately polished discs; these served as substrates for the majority of the work that was subsequently performed.

Electron microscopy data obtained at NRL provided conclusive evidence of second-phase formation in boron-implanted beryllium samples.[23] The diffraction results suggested that more than one beryllium boride phase was possibly present. Since the temperature during implantation was intentionally held to low values, the increased boron mobility, as indicated by the ocurrence of precipitate formation, was in all likelihood the result of irradiation-enhanced diffusion. The presence of a multitude of phases might well have been the result of localized compositional variations in the implanted specimens.

4.3.2.2 Chemical Analyses

Because of the many difficulties encountered earlier with obtaining sharp, well-defined diffraction patterns using RED with the view of providing detailed information on beryllium-boron compound formation in the implanted layers, subsequent efforts were mainly directed at examining the implanted materials using the Rutherford Back Scattering (RBS) and the Auger Electron Spectroscopy (AES) techniques for chemical composition analysis. Since both these techniques are capable of determining composition depth profiles, they were both pursued with the aim of establishing correlations between the use of these two different analytical procedures. The RBS data were collected at NRL. AES, however, was performed locally under CSDL direction.

4.3.2.2.1 Rutherford Back Scattering (RBS)

Rutherford back scattering was performed using 3-MeV alpha particles incident at 45 degrees to the surface normal and at 90 degrees to the detector. Because the kinematical scattering factors for boron and beryllium do not differ sufficiently to separate the signal from the deeply buried boron from that of the near surface beryllium, the determination of the boron profile involved elaborate techniques. First, a spectrum from an unimplanted specimen was subtracted from the spectra of the implanted samples. (The resulting difference spectrum had the advantage of being less sensitive to the choice of beryllium

cross section.) Then, an RBS simulation computer code was used to generate a theoretical difference spectrum which was compared to the observed difference spectrum. The matching process involved adjusting the concentration profile input to the code until the best fit to the observed data was achieved. The final form of the profiles, as obtained using RBS, for the flat and graded distributions of 40 atom percent boron peak concentration samples are shown in Figure 5.

It was estimated that the uncertainty in the boron concentration was 15 to 20 percent of the plotted values. The depth scale was less certain since the back scattering technique is sensitive only to the number of boron atoms per atoms-per-unit area and is insensitive to the local atomic density. Is was expected, therefore, that the true distributions might differ from those in Figure 5 by some expansion or contraction along the depth axis.

4.3.2.2.2 Auger Electron Spectroscopy (AES)

Auger evaluation of the implanted materials was performed using a Physical Electronics Model 590 machine, The machine was operated at 5 kV and the spot size of the incident electron beam was slightly less than about 1 μm. Depth profiles were obtained by sputtering the sample with argon ions and simultaneously examining the chemical composition of the material that was exposed to the incident beam at the various depths. The data was plotted on a chart recorder with the concentration (as indicated by the peak-to-peak amplitude) of the several atomic species of interest on the vertical (y) axis and the time of sputtering on the horizontal (x) axis. Since the rate of sputtering of the implanted layer was not known, it was not possible to relate the time of sputtering to the depth attained inside the sample by simple conversion of the data.

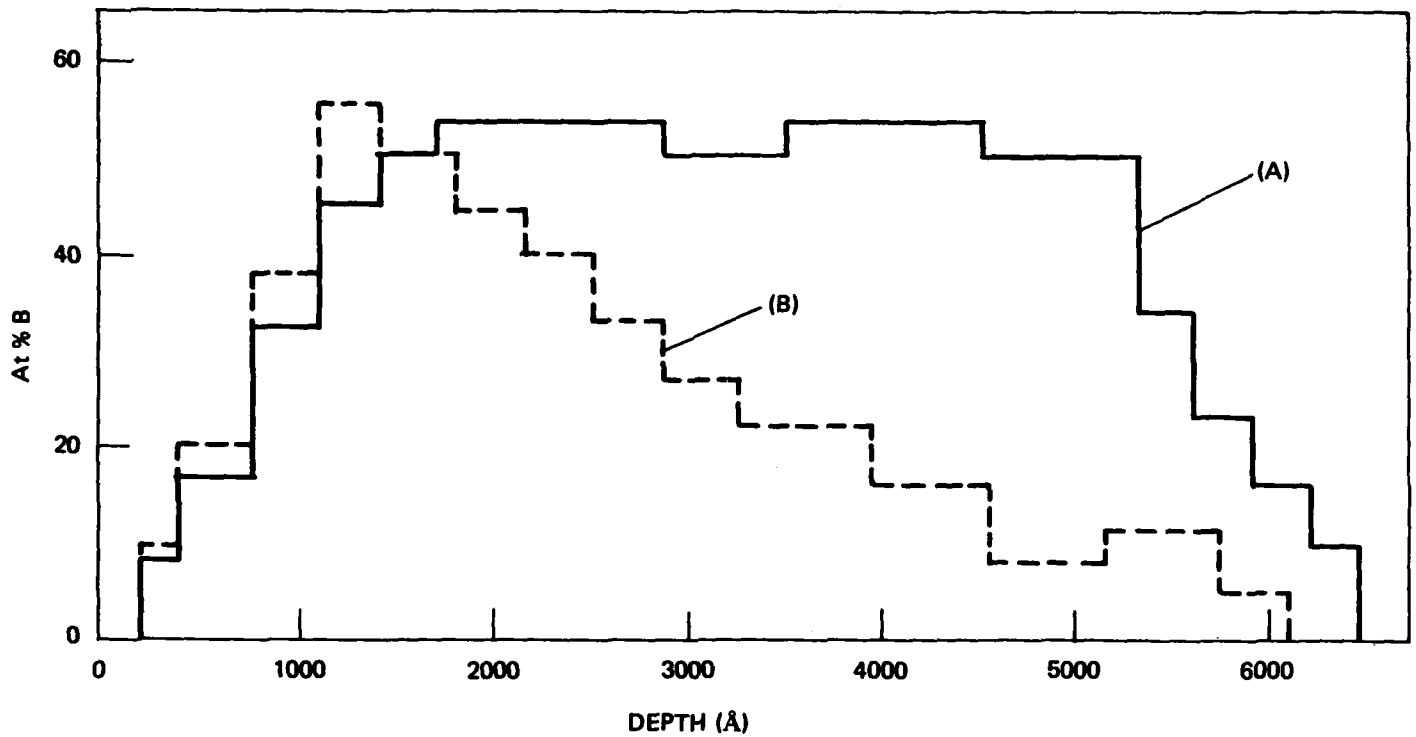

Figure 5. RBS concentration profiles of (A) flat NRL 40-V, and (B) graded layer NRL 40-VI samples.

To more accurately determine the concentation profile, as stated in the previous section, an alternate method was devised. This consisted of measuring the depth of the groove (that was formed by sputtering of the sample surface) with a Sloan Dektak surface profilometer and assuming that the rate of sputtering was a constant throughout the sputtering period. A given fraction of the groove depth was, therefore, equivalent to the same fraction of the sputtering time.

AES profiles measured for NRL implanted peak 40 atom percent boron flat and graded profile specimens are shown in Figures 6 and 7. The measured profiles were close to what was expected on the basis of the RBS data shown in Figure 5. These data were not normalized because of lack of information on the relative sputtering rates of boron and beryllium. A close correlation was observed between the RBS and the AES data, clearly establishing the feasibility of using AES (which was more accessible) for purposes of evaluating sample composition and depth profile.

4.3.2.3 Friction and Wear Evaluation

4.3.2.3.1 Test Results

Much of the early friction and wear data was obtained using a pin-on-disc format with pins made from 52-100 steel. The tests were performed on freshly cleaned surfaces without lubricants or coolants, as a means of ensuring well-defined and reproducible conditions. Perhaps because of the absence of any lubricating film, in many instances the steel pin material "crayoned" itself onto the disc surfaces resulting eventually in steel rubbing on steel. This occurrence, plus the desire to generate data with more direct engineering value, led to the recommendation that further wear and friction evaluation be performed with materials of potential use in gas bearings, such as an aluminum oxide (sapphire)-tipped pin.

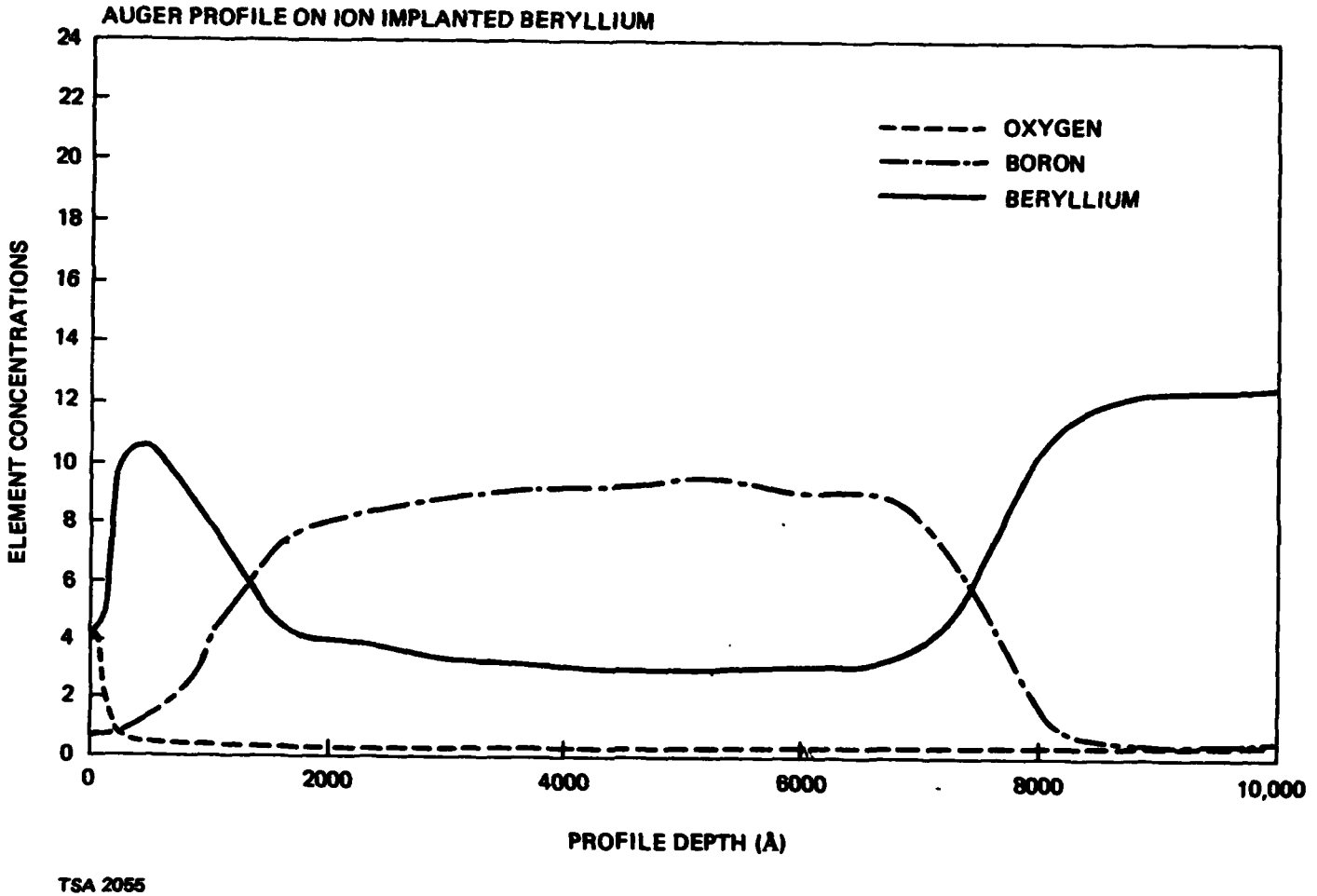

Figure 6. Depth concentration profile of NRL flat distribution sample (NRL 40-IV).

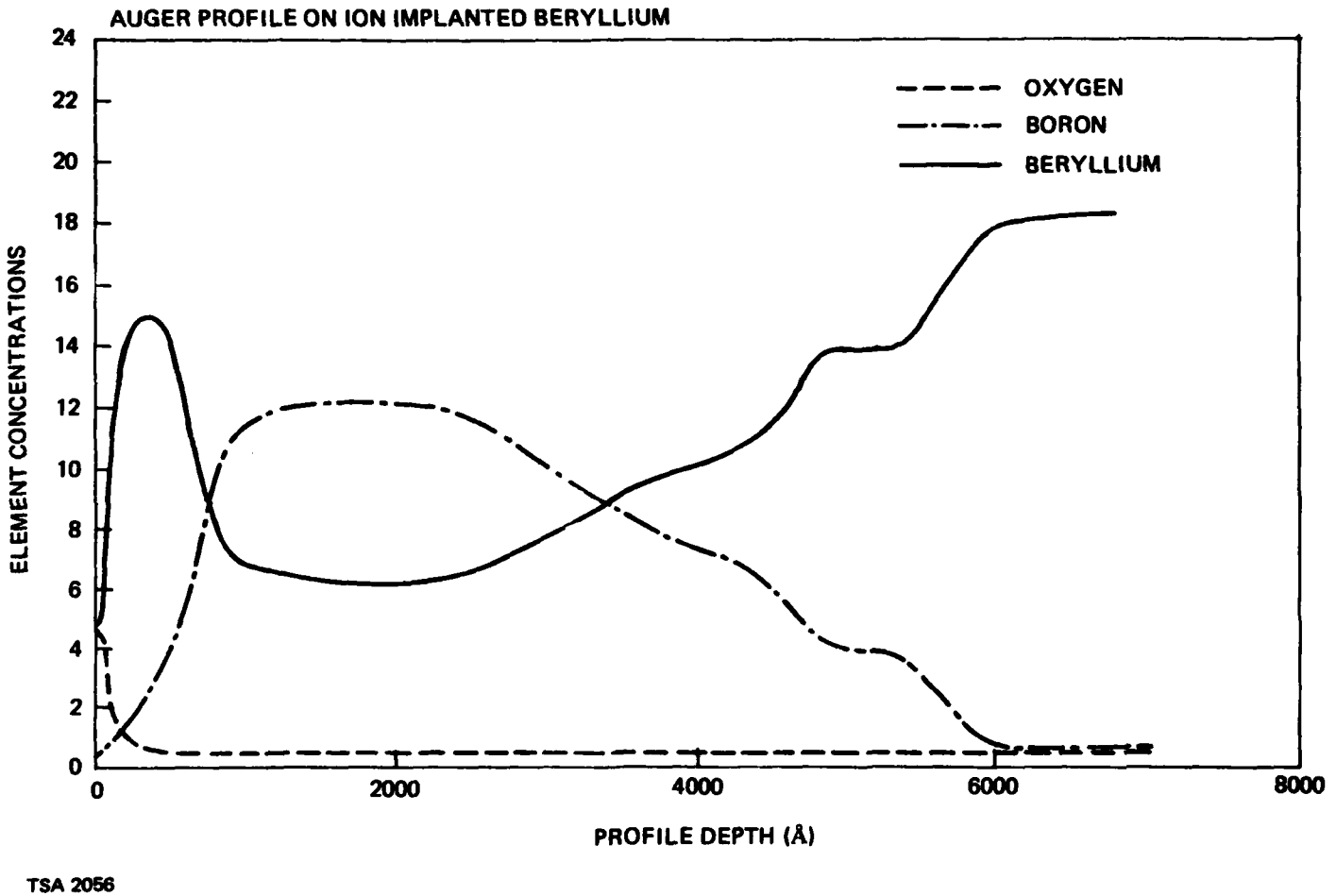

Figure 7. Depth concentration profile of NRL graded distribution sample (NRL 40-VII).

The additional wear testing was also performed using the pin-on-disk technique with the CSDL-designed flex pivot wear-tester.[20] The tests were performed at 100 r/min for 10 minutes duration. Pins used included a 3.2-mm sapphire ball installed in a steel cylinder and a beryllium-titanium diboride composite cylinder with its end ground to the same radius of curvature. The samples were wear-tested with progressively higher loads applied to the pin to give a relative measure of performance. Optical micrographs were taken of the wear tracks generated at the increased loads.

Table 4 summarizes the friction coefficient data obtained with a 20 g applied load.[24] The peak intended boron concentrations of the different samples are shown in parentheses in the second column of this table.

The most repeatable values for μ were obtained at loads below which no evidence of a wear track could be detected with a Dektak surface profilometer. In most instances, applied loads of about 20g showed little or no evidence of a wear track. The data using the sapphire pin indicated that even at the lowest (10 percent) boron levels, the initial friction coefficient was significantly lower than that measured for unimplanted beryllium,[19] and that this value was relatively constant for short duration (approximately 0.1 sec). Figure 8 illustrates the observed effect of increasing the applied load on the coefficient of friction. This observed effect of the load on the friction traces was explained in the following way. The boron depth profiles indicated that little or no boron existed in the region near the surface of the implanted samples. The initial low and constant values of μ (measured for all the compositions that were investigated) were, therefore, possibly associated with increased wear resistance imparted to the surface by radiation damage from the penetrating boron ion flux. This reasonably boron-free beryllium surface layer was destroyed with increase in time of test and/or increased load, during which time the friction coefficient registered a reasonably rapid increase.

Table 4. Measured values of the friction coefficients at different times for the several wear runs.

Specimen	Profile	μ (20 g load)				Load Causing Severe Damage in Wear Region
		Actual (Intended)	Sapphire		Composite	
			0.1 Min	1 Min	1 Min	
1	G	20(10)	0.14(3)**	0.21(3)**	-	30g
2	G	35(20)	0.15(20**	0.20(2)**	-	>40g
3	G	45(30)	0.14(3)**	0.26(3)**	-	30g
4	G	55(40)	0.16(4)**	0.21(4)**	-	50g
5	F	55(40)	0.15(6)**	0.15(6)**	0.46	60g with sapphire; up to 110g with composite
Be (anodized)	-	-		0.66	0.30	50g
1HT	G				0.53	30g
2HT	G				0.39	60g
3HT	G			0.22	0.63	60g

G = Graded; F = Flat; HT = Heat Treatment = 450 °C, 1-1/2 hrs.

** Number in parentheses indicated that the reported friction value was measured and averaged over that number of runs. Other data reported were based on a single run.

$W_1 < W_2$.

$\mu_{measured} = \mu_T + \mu_W$,

where μ_W is dependent on wear of the surface, and

μ_T = true value of the friction coefficient.

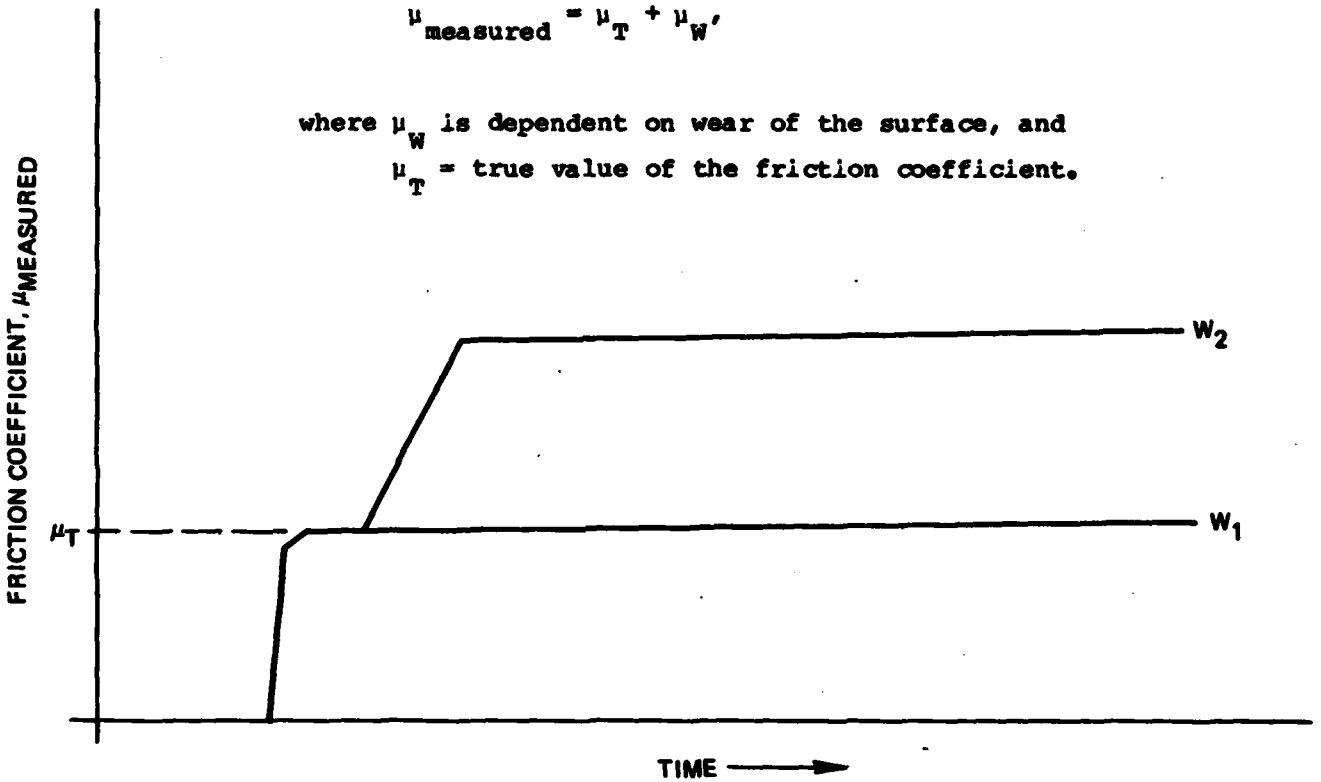

TSA 2057

Figure 8. Schematic showing observed effect of increases in applied load on characteristics of friction trace of implanted beryllium.

Additional wear was very gradual through the boron rich layers. This latter effect appeared in the form of a very slowly increasing value of the friction coefficient with time. Somewhat surprisingly, this rapid stepped increase in μ was not noticed with the composite pin tests. The higher friction coefficient values that were measured were considered an indication that the microscopically rough surface of the composite pin possibly removed the boron-free beryllium surface quite rapidly to be sensed by the instrumentation. Inconsistency in μ at the 0.1-minute interval with the composite pin required tabulation at the 1-minute duration; the sapphire data obtained at 1 minute is, therefore, also included for comparison.

4.3.2.3.2. Optical

Although the initial (0.1-second duration) μ values, for the sapphire pin, were roughly the same for all of the specimens, the wear resistance over full 10-minute intervals was quite different for various implanted conditions. Figure 9 depicts the wear tracks observed on samples 1, 2, and 3 after 10 minutes of test using a sapphire pin at 30-gram load. Severe wear (i.e., significant debris, rugged wear track) was found to have been initiated in samples 1 and 3. However, even at 40 grams, sample 2 showed no such signs. The reasons for this anomalous behavior of sample 2 were not clear. As indicated in Table 4, after heat treatment, sample 1 HT showed severe wear at the same 30g level with the composite pin; samples 2 HT and 3 HT survived to the 60-gram load level. This was an improvement after heat treatment for sample 3. It was considered possible that the heat treatment flattened the highly graded profile of sample 3. It was concluded that flat profile samples showed superior wear resistance compared to graded samples. Of all the several samples that were evaluated, the 40 atom percent boron flat profile samples were found to possess the maximum resistance to wear. This study also demonstrated that the composition of the layer, a given distance below the actual wearing surface, determined the resistance of that surface to further wear. Further study on 40 intended atom percent flat profile samples showed inconsistent results as to resistance to

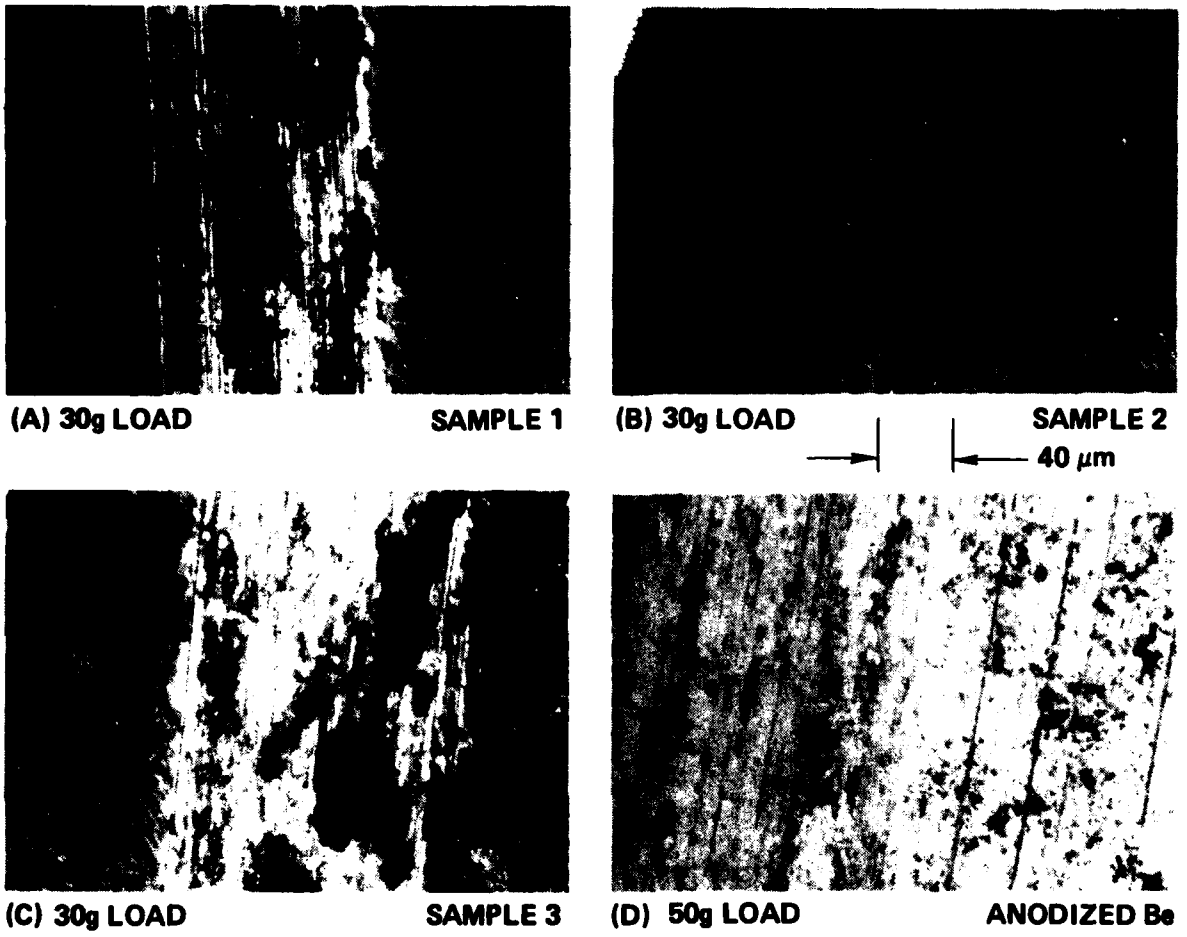

Figure 9. Wear tracks observed at indicated loads. Samples 1, 2, 3 contacted a sapphire pin. The anodized beryllium sample was run against a Be-TiB_2 composite pin.

severe wear. One sample showed absence of severe wear even after a 110-gram loading with the composite pin.

Experiments performed with the composite pin on an anodized beryllium surface exhibited signs of severe wear after a 50-gram loading (Figure 9D). A low μ value was measured for this sample. However, the surface was lubricated prior to the measurement. This was believed to have been responsible for the low value.

4.3.2.3.3 Microhardness Measurements

The hardness of a surface is generally considered an indication of its wear resistance. Therefore, the higher the hardness, the greater would be the expected wear resistance. Microhardness values in Knoop Hardness Numbers (KHN) (expressed in kg/mm^2) made on several of the samples are shown in Table 5. [It was difficult to measure the hardness of such thin surface regions accurately. At high applied indentation load the substrate contribution was excessive. At very low loads the surface contribution dominated but questions arose with respect to "the actual" as compared to "the intended" load. We therefore devised a procedure whereby microhardness measurements were made over a range of applied loads. The variation of microhardness as a function of applied load provided a more reliable assessment of the hardness of the surface.[18]] Conventional thinking notwithstanding, the data in Table 5 showed that the wear behavior of these samples could not be explained on the basis of the measured microhardness data.

Table 5. Average microhardness readings KHN (Kg/mm^2) on several implanted samples.

Applied Load (g) \ Sample	1	2	3	4	5
50				341	356
25	372	381	390		
10	703	643	686	762	542
5	1123	1017	1184	1211	1153
2	1736	1682	1622	2233	1965

4.3.3 Hardware Fabrication and Evaluation

Because the wear test experiments performed in this program showed that the 40 atom percent boron flat profile gave the best results, two beryllium discs, with grooves in place, were implanted with this concentration and profile to examine the industrial applicability of the implanted surfaces for actual gas bearing use. These two discs constituted the thrust plates of a conventional spool-type gas bearing. To minimize the number of variables, all of the other structural members, including the rotor and the journal were selected from existing hardware with only the boron-implanted thrust plates comprising the change. The bearing was assembled unlubricated, in contrast to the conventional bearing which has a lubricant applied to its rubbing surfaces prior to evaluation and performance, and tested as a gas bearing. The response of this modified gas bearing was very satisfactory during the initial evaluation with respect to start-up and touchdown characteristics. When the bearing was examined for life test performance in regard to repeated start-stop cycles, the bearing was observed to fail after a few cycles. When the bearing was disassembled for inspection, it was discovered that the failure was related to removal of a small chip off of the anodized surface of the journal. The implanted thrust plates looked as good as new.

A new set of parts was subsequently received for assembling another bearing with the same thrust plates. Once again the bearing was assembled without lubrication and evaluations performed. The initial response of the bearing was deemed acceptable, even though high touchdown speeds were observed. High speeds were believed to have resulted from a slight mechanical distortion of the bearing journal that was associated with the particular fixture that was used. The bearing was then examined for life test performance through evaluation of the bearing condition during start-stop testing. The results were found to be extremely promising in that little or no degradation in physical integrity of the various bearing parts (as well as in bearing characteristics) was observed along the two axes tested, from a total of 5000 start-stop tests performed along each axis.

Tests were also performed, in conjuction with a commercial vendor, to evaluate the suitability of combining this technology with that for the Be-TiB_2 composite discussed in the next section. The results were found to be quite promising in this respect as well.

SECTION 5

COMPOSITE MATERIAL

5.1 Introduction

Beryllium-ceramic metal matrix composites fabricated by hot isostatic pressing of blended powders were examined as an alternate approach to the fabrication of hard, wear-resisting surfaces for use in gas bearings. Beryllium served as the metal matrix in these composites because of its very desirable bulk properties. The physical properties of a composite made from this metal were, therefore, expected to be more compatible to the rest of the gyro structural members than those either of a solid ceramic or of composites fabricated using other metal constituents as the host material. (The wear and friction process in these materials is confined to the ceramic particles standing out in relief at the surface of the composite.)

The Be-TiB_2 composite developed in this program has continued to show promise as a gas bearing material. As with the boron implantation effort, this technology was also transitioned into specific hardware programs. Lapping studies showed that flatness and smoothness of the composite surface, to within bearing specifications, were possible with minimal damage to the ceramic particles. Even though the measured values of the thermal expansion coefficient of the composite were subtantially lower than that of beryllium, the values achieved were considered acceptable for several designs in view of similarly low expansion materials that have been previously used.

5.2 Goal

As in the previous two subtasks, the goal here also was to provide for a surface that would demonstrate high wear resistance and low friction from rubbing processes. This was to be accomplished

through incorporation of ceramic particles within a beryllium matrix, the purpose of which was to limit the wear and friction process to the ceramic particles standing out in relief at the composite surface.

5.3 Results and Discussions

Work performed in this subtask emphasized the following broad areas:

(1) Composite development

(2) Lapping procedures for definition of microstructure and production of acceptable bearing surfaces

(3) Wear and friction behavior, and

(4) Production of near-net shape parts for minimizing cost

The results achieved in each of these areas is described in what follows.

5.3.1 Composite Development

5.3.1.1 Material Selection

The criteria that were used to select ceramic powders for fabricating these composites included the following:

(1) Microhardness

(2) Chemical stability, and

(3) Thermal expansion compatibility

A ceramic with a high value of microhardness was desired principally because hard materials are known to be resistant to degradation from processes such as impact and erosion and also because these display relatively low values for the coefficient of friction.

Chemical stability, as indicated by the values of the free energies of formation of the several compounds, is of concern during consolidation because even though it is important that the metal matrix wet the ceramic, one does not want the metal to chemically reduce the ceramic at the temperature used for densification.

Thermal expansion compatibility consideration involves selection of a ceramic with an expansion coefficient only slightly lower than that of the surrounding metal as this leads to a mild compressive state of stress around the particle. An expansion coefficient higher than the metal will cause the ceramic particles to pull away from the metal during cooling after hot consolidation, whereas one considerably lower will result in a very high level of stress.

Because of these several theoretical considerations, three different types of ceramic powders were initially selected to separately form the composite with beryllium. The ceramics selected were Al_2O_3, TiC, and TiB_2.

5.3.1.2 HIP Process Development

5.3.1.2.1 Initial Experiments

Be-TiB_2 composite material fabricated (during initial experiments) using the hot isostatic pressing technique demonstrated that the fabrication sequence in itself needed a certain amount of development effort. The micrograph in Figure 10(A) shows the poor densification obained in a sample that was isostatically densified at 900°C temperature and a 15-kpsi gas pressure for 2 hours. Large pockets containing loose TiB_2 powder were observed with the unaided eye. The

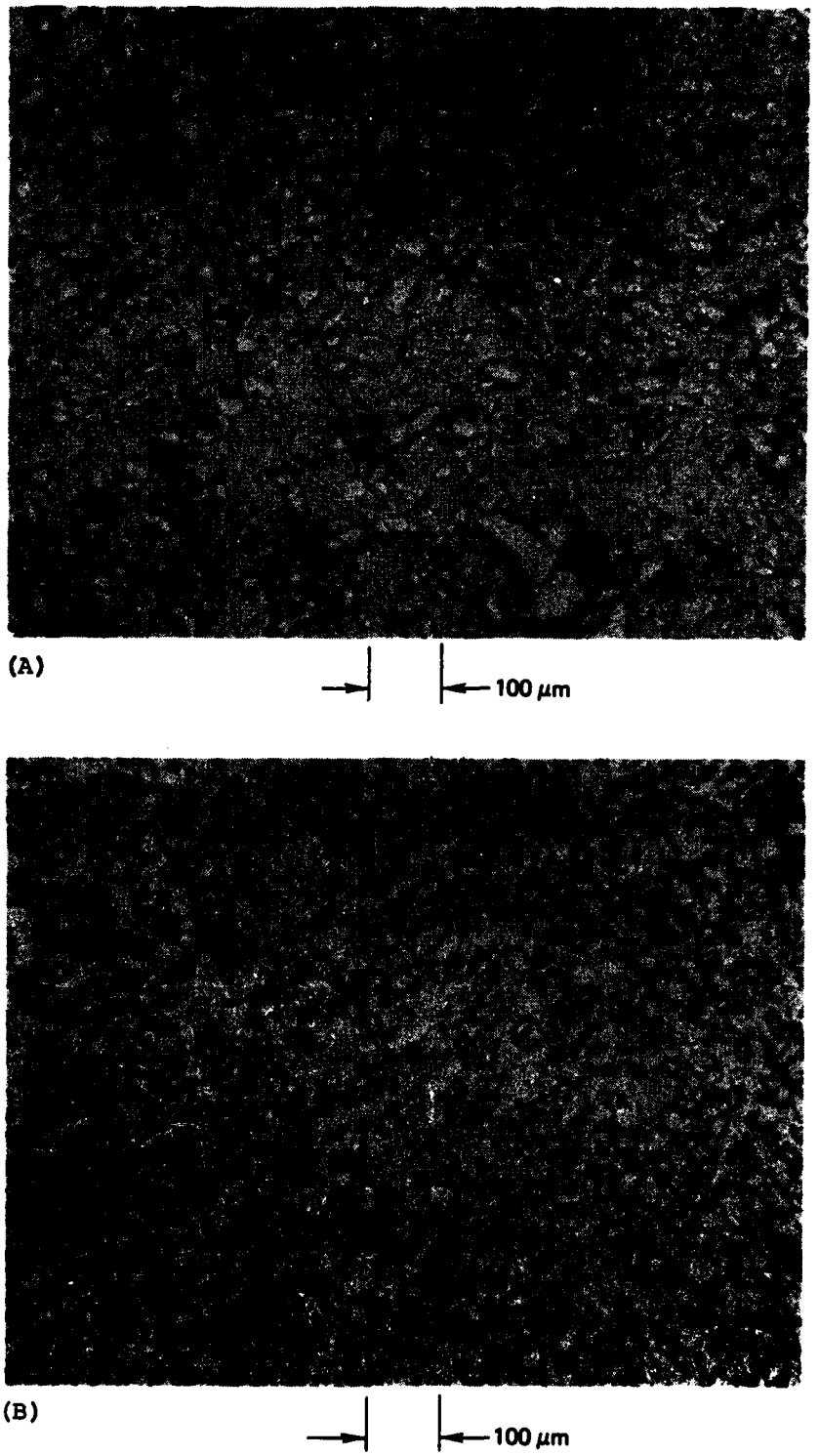

Figure 10. TiB_2 dispersion in Be matrix. (A) Poor densification and dispersion; (B) improved densification and dispersion. As polished.

observed defects were attributed to poor blending (which was done by a gentle tumbling action using a conventional laboratory blender), insufficient outgassing of the powders (which was performed at 400°C prior to sealing the powder compacts in metal cans before densification) and a possibly lower than optimum densification temperature (900°C in this experiment). This problem was subsequently corrected by resorting to higher energy powder blending (in a ball mill), outgassing of the powders at 600°C prior to container excapsulation, and use of a slightly higher densification temperature (950°C) for an equivalent length of time. The improvements in structural uniformity and material integrity that resulted from these steps are evident in the photograph shown in Figure 10(B). The variation in observed ceramic grain size in these micrographs is attributed to the selection of the starting ceramic powder, designated as -325 mesh, or less than 45 μm, therefore indicating a wide range of particle sizes.

5.3.1.2.2 HIP Fabrication of Samples

Beryllium powder, designated as -325 mesh, was procured commercially and blended with selected samples of the different ceramics (Al_2O_3, TiC, and TiB_2) using the high energy blending procedure discussed above. Ceramic powders were obtained in two different sizes of -325 mesh (less than 45 μm) and 1 to 2 μm from a commercial source. The ceramics were separately mixed with the beryllium to yeild powder blends containing 40 and 55 vol% of ceramic. The blended powders were then placed inside rubber boots and cold isostatically pressed at a pressure of roughly 60 kpsi. All of the beryllium handling was performed in a hood specifically designed for such purposes, while adhering to strict safety procedures.

The green compacts, obtained after cold isostatic pressing, were encapsulated, under vacuum, in low carbon steel containers and hot isostatically pressed for 2 hours at a temperature of 975°C and an inert gas pressure of 15 kpsi in a high-temperature autoclave.

One of the more noteworthy observations made during this study is shown in Figures 11 and 12 and is related to micromachining effects observed on -325-mesh TiB_2 particles and differences in ceramic particle distributions in the composite.[25,26] These SEM micrographs show that whereas the -325 mesh samples showed a reasonably uniform distribution of the particles throughout the beryllium matrix, the 1- to 2-μm samples showed that the ceramic particles were mainly segregated at the grain boundaries of the beryllium. Also, the 1- to 2-μm ceramic particles were not completely surrounded by the beryllium as compared to the -325-mesh particles which showed an intimate physical contact between the ceramic and the beryllium (all around the ceramic particle). Micromachining effects on the ceramic particles were not observed in the 1- to 2-μm samples, possibly because of their very small particle size, and a lowered tendency of the particles to remain bonded to the matrix.

Another significant observation made during these investigations was the near absence of micromachining of the ceramic particles in the -325-mesh, Al_2O_3-containing composite. The SEM observations on the as-lapped condition of this composite showed the existence of reasonably large voids in sizes comparable to the -325-mesh Al_2O_3 particles. These voids were concluded to have resulted from Al_2O_3 particle pullout during the several lapping operations the composite was subjected to during disc sample preparation.

Of the three ceramics (Al_2O_3, TiC, and TiB_2) that were investigated, TiB_2 appeared to be the best suited for forming of the beryllium-ceramic composites. Al_2O_3-containing composites possessed the severe deficiency related to poor bonding of the Al_2O_3 particles to the beryllium matrix and the TiC-containing composites could not be HIPed to high density. Microstructure observations showed that the low density

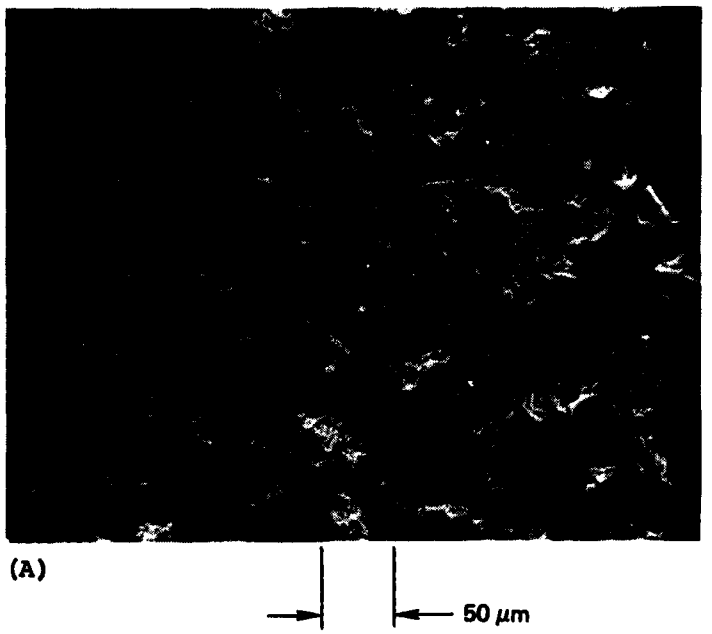

Figure 11. SEM photograph of 35 vol.% TiB_2, - 325 mesh TiB_2 composite. Lapping resulted in micromachining effects on ceramic particles. (A) As-polished; (B) after 2 seconds KBI etch.

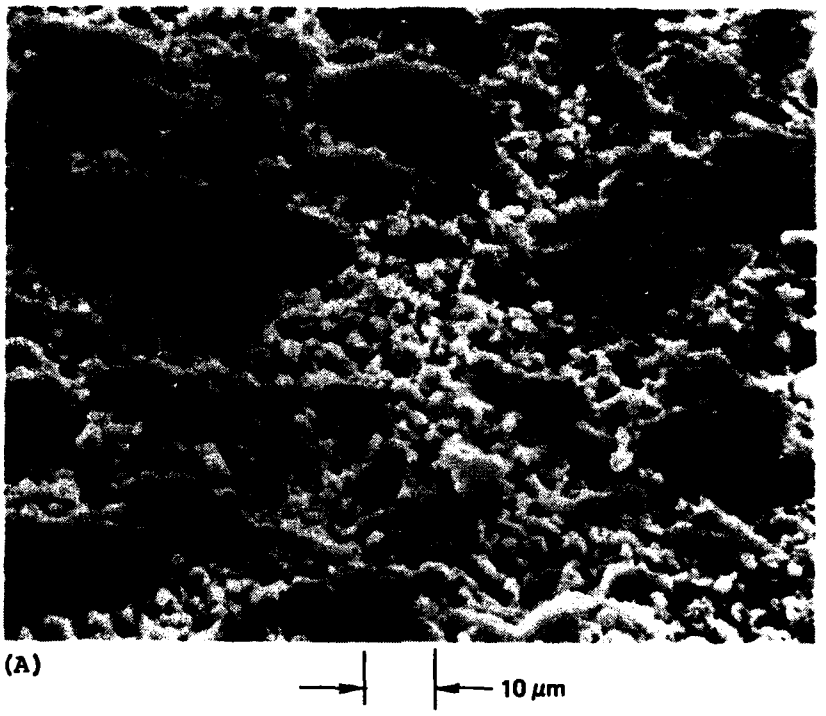

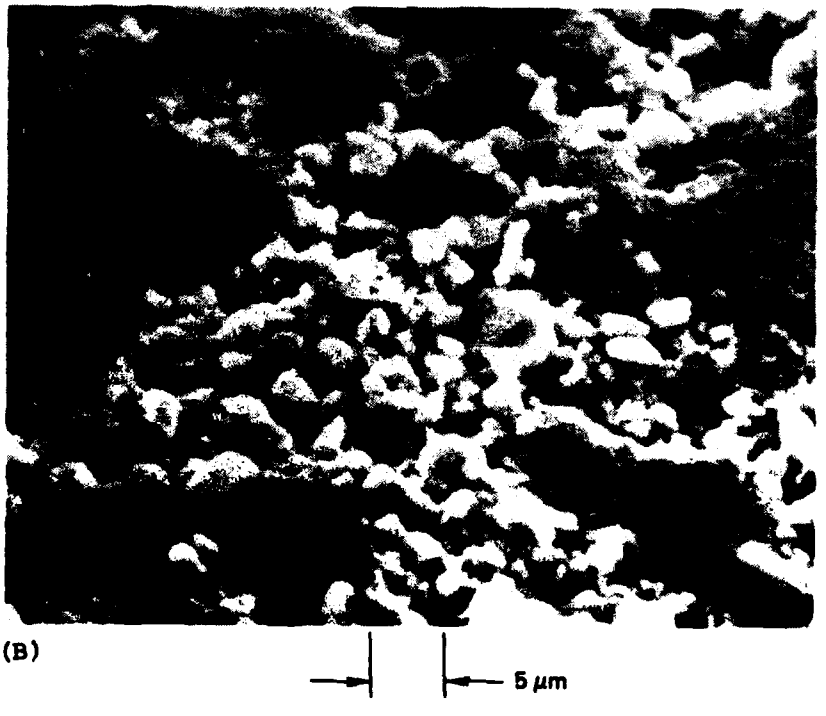

Figure 12. Higher magnification SEM photographs of 40 vol% TiB_2, 1-2 μm particle size sample. TiB_2 particles are clearly observed in grain boundary regions.

values observed for the TiC-based composites were related to difficulties in outgassing of the TiC powders prior to HIP processing.

All of the subsequent evaluations were, therefore, performed on TiB_2-based composites.

5.3.2 Lapping Studies

Initial observations on effects arising from the lapping of these materials were made on discs made from a 35 volume percent TiB_2-containing composite sample that was produced earlier. These studies showed that use of coarse (500-grit size) particle Al_2O_3 as the lapping medium resulted in the ceramic particles standing out considerably in relief above the beryllium surface. Scanning Electron Microscopy (SEM) observations showed that the surface of the recessed beryllium after polishing with coarse particles was quite rough after this polishing procedure. When this sample was subsequently polished with the finer Al_2O_3 paste (the finest contained a 2-to 3-μm Al_2O_3 particle size) micromachining of the TiB_2 particles was observed. This is believed to have continued until the height of the ceramic particles was reduced to that close to beryllium, beyond which point both the beryllium and the micromachined ceramic particles were subjected to a simultaneous polishing action. SEM observations relating to the micromachining effects discussed above are shown in Figure 11. Figure 11 also contains a photograph obtained on this sample after selectively dissolving the beryllium (relative to the ceramic) for about 2 to 5 seconds using a KBI etch.* Figure 11 suggested that the step height between the beryllium and the ceramic could possibly be adjusted by varying the time of etching.

---

* KBI etch consists of 500 ml H_2SO_4 + 500 ml phosphoric acid + 750 g chromic acid + 3 l water (use at 50°C). Developed by Kawecki Berylco Co.

Whereas good definition of the microstructure was obtained by the techniques noted above, these were, nevertheless, inappropriate for producing surfaces for use in gas bearings. The limitiations on the use of the above procedure(s) included (1) not being able to produce extremely flat surfaces, (2) the average roughness of the polished surface was at least several times coarser than what would be considered acceptable, and (3) sample polishing involved an inordinately long operator time, thereby making the process less attractive for production purposes.

Hand-held lapping procedures, which included polishing of the TiB_2 composites using diamond laps, resulted in producing surfaces that were both flat as well as having acceptable values of surface roughness. The ceramic particles, however, were severely damaged with this process. Figure 13 shows a typical surface that was produced using diamond polishing. Comparison with the surface shown in Figure 11 clearly shows the extent of the damage that had occurred to the TiB_2 particles. When a set of gas bearing parts that was lapped in this manner were cleaned using ultrasonic means, it was observed (at a vendors facility) that continuous particluate generation resulted during the cleaning process. This raised concerns as to whether these parts could ever be cleaned thoroughly and whether continuous particulate generation was indicative of poor mechanical integrity of the material that might lead to catastrophic deterioration of the gas bearing during operation.

A reasonably detailed examination, was, therefore, performed on an experimental part to confirm whether cleaning of the material using ultrasonic means indeed resulted in degradation of the material. The experiments consisted of examination of a few selected areas on the as-received part. These were readily identifiable in that there were local areas of damage introduced during the earlier lapping process. Subsequent examination of these same areas was performed each time after ultrasonic cleaning.

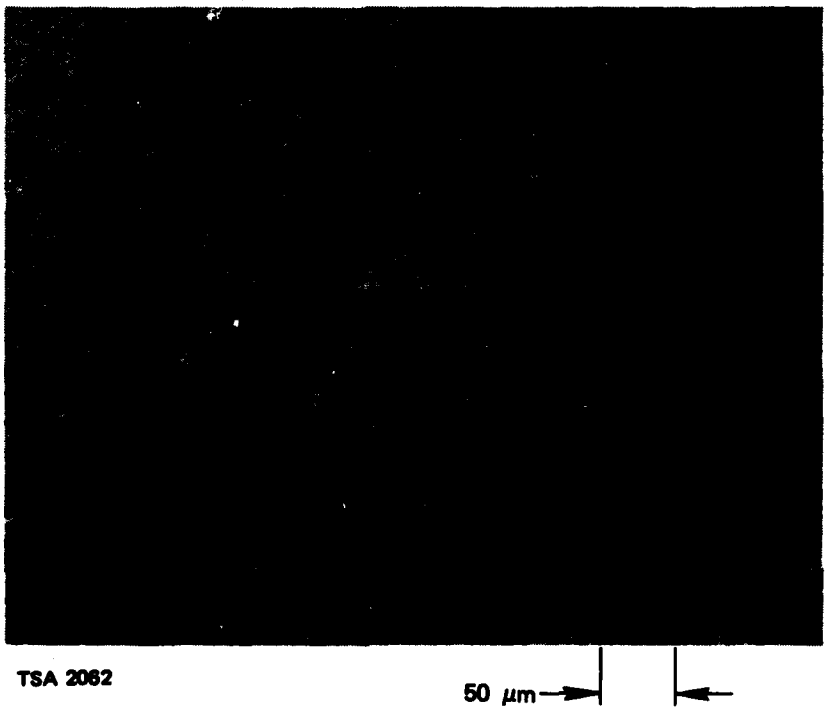

Figure 13. As-lapped diamond surface. 45 vol% TiB_2, - 325 mesh composite.

Observations typical of what were made are shown in Figure 14. In Figure 14 the micrograph designated as (A) corresponds to the as-received condition, (B) the same region after 10 minutes of ultrasonic cleaning, and (C) the same region after an additional 20 minutes of cleaning (i.e., a total of 30 minutes in the ultrasonic cleaner). These micrographs indicated that in each instance, the minor changes that were noted had all occurred in the small pockets of damage that were present. The remainder of the material remained unchanged. These observations suggested that the composite parts should be cleaned as thoroughly as possible and fabrication procedures be developed that would minimize defect regions in the material. It was also suggested that substantially more care be exercised during the lapping process so as to drastically reduce, if not altogether eliminate, the occurrence of the pockets of damage that were observed. Additional cleaning experiments performed on composites containing fine (-10 μm) and coarse (+30 μm) TiB_2 particles further suggested that the coarse particle composites were less susceptible to particulate generation than were the fine particle composites, in agreement with the less than optimum bonding observed earlier for fine TiB_2 particles within the beryllium matrix.

Reasonably extensive hand-held lapping procedures (primarily using diamond containing compounds and diamond impregnated commercially procured Abernathy laps) were subsequently investigated with the purpose of producing well-polished TiB_2 surfaces in relatively short time. It was noted, in agreement with earlier observations, that severe damage (which was observed as pits) resulted in the ceramic particles from contact with the diamond particles. When polishing using fine particle (0.05 μm) Al_2O_3 was attempted on these surfaces, gradual removal of damage was observed; however, this was obtained at the expense of producing a considerable amount of ceramic particle relief at the surface. This problem was substantially minimized when Syton (a commercially available ultrafine particle SiO_2 suspension) was used as the polishing medium. The damage to the individual ceramic particles was substaintially removed by this technique.

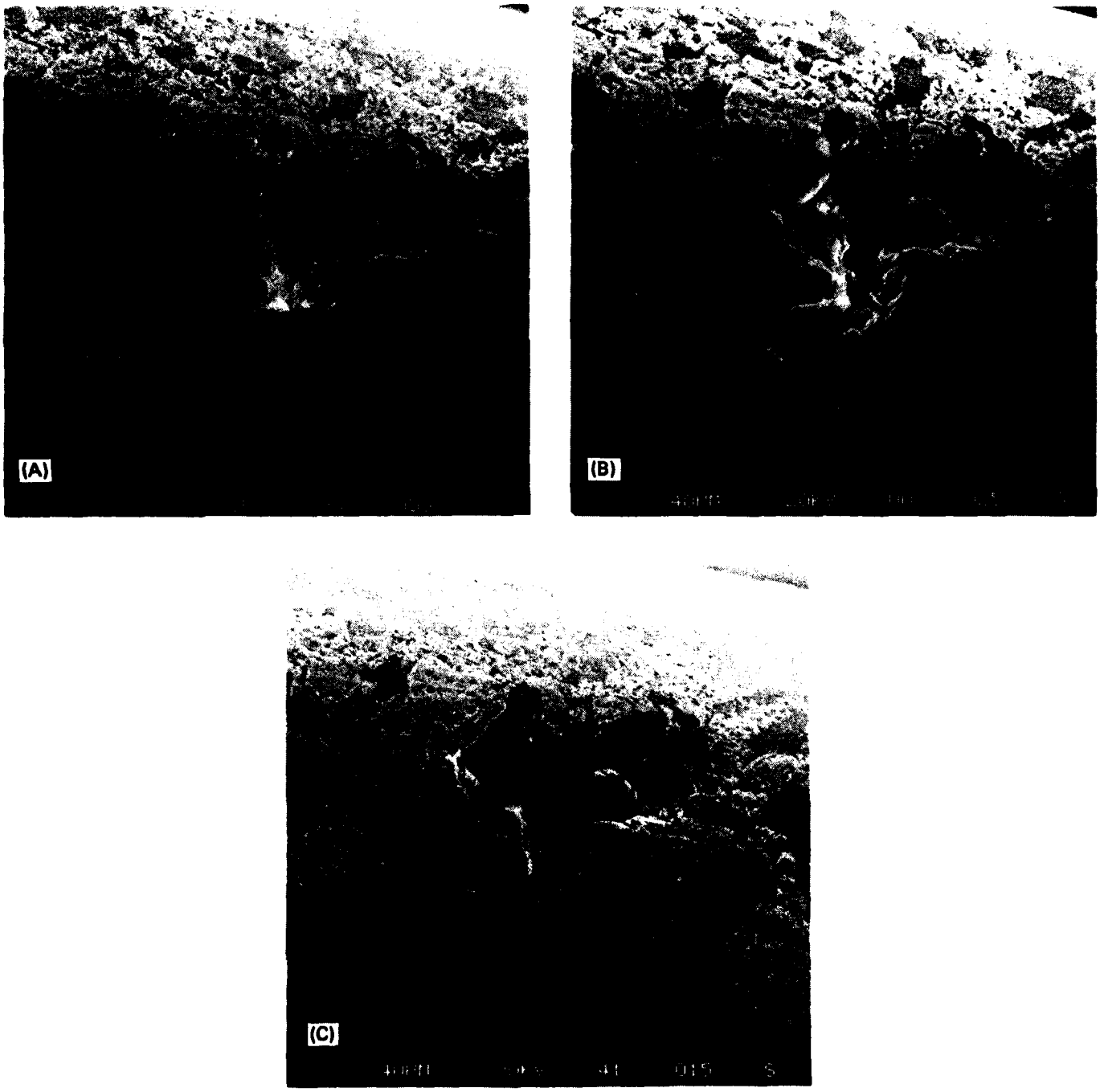

TSA 3105

Figure 14. Two large particles in (A) and (B) are removed in (C). No changes in surrounding areas.

While these revised procedures resulted in surfaces which contained damage-free ceramic particles, the surface roughness was still excessive. This was attributed to the relatively long exposure to Syton polishing that was performed on a Polytex (cloth) wheel. The surface roughness as well as surface flatness concerns were subsequently addressed by additional modification and development of the lapping process to include machine lapping procedures such that the process could be used for production purposes. This latter work was performed with a composite having TiB_2 particles in the +20- to -30-μm size range.

The new, revised procedure that was found to be reasonably successful included machine lapping (of previously diamond-lapped parts) with Al_2O_3 followed by short-time hand lapping with Syton. Machine lapping was performed using a mehanite lap and a 3-micron Al_2O_3 charge which was drip-fed onto the lap to maintain a wet look. The surface was lapped to obtain a surface with better that a 4-microinch finish. The sample surface was then cleaned and polishing of the ceramic particles performed using Syton polishing on a Polytex cloth mounted on top of a flat plate. The surfaces produced during different stages of the lapping/polishing process are shown in Figure 15. Figure 16 contains traces that show the surface topography (including the peak to peak variation), which gives the amount of roughness present in the sample. This data was obtained using a Dektak Surface profiling apparatus. This variation was found to be about 6 to 8 microinches after Al_2O_3 lapping (of the diamond lapped part) for 1 hour. The surface roughness observed after polishing it with Syton for 1-1/4 minutes was found to have the superior value of about 1 to 2 microinches which was in the acceptable range for gas bearing surfaces. It should be noted that this surface was not very flat and this was believed to be associated with the particular lap that was used. It was felt that by going to an improved lapping machine this situation can be corrected. This belief was reinforced by the observation that even though the surface roughness did improve with the procedures that were followed, little significant alteration in the flatness was observed for this sample.

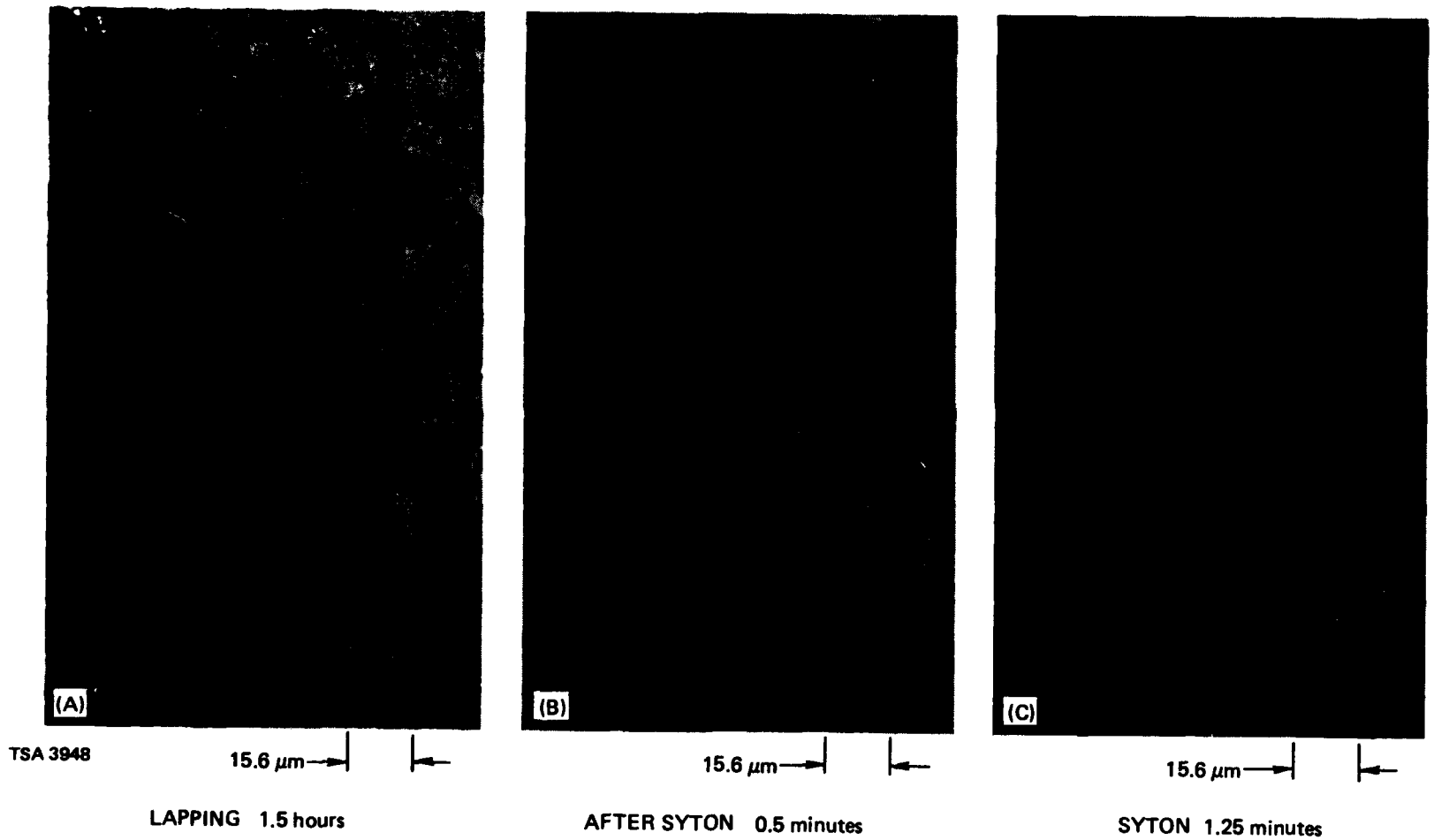

Figure 15. Nomarski photographs obtained after (A) Al_2O_3 lapping; (B)(C) Syton lapping for times indicated.

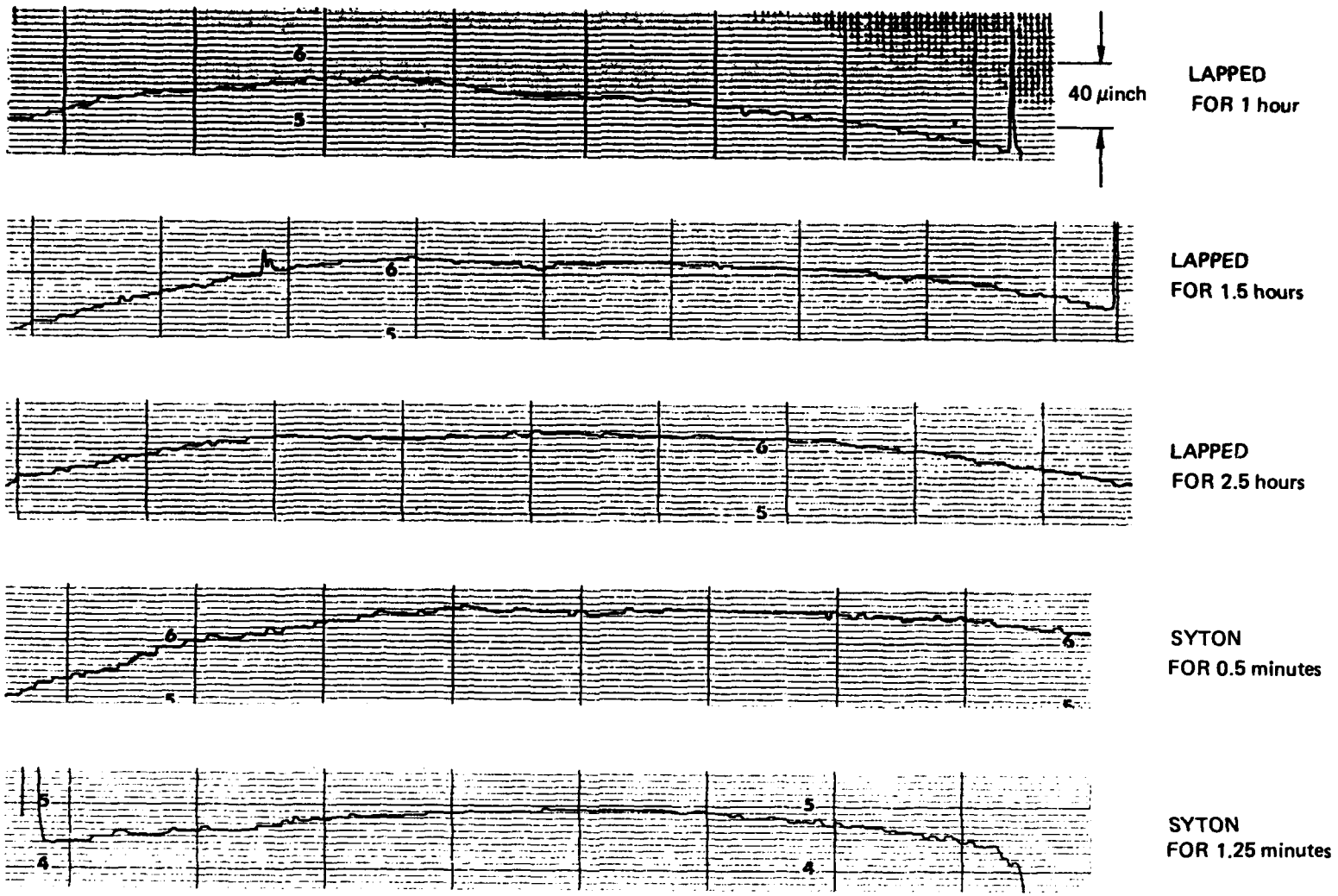

Figure 16. Dektak surface profiles obtained on composite sample after lapping (with Al_2O_3)/polishing (with Syton) steps as indicated.

5.3.3 Wear and Friction

Wear tests were performed using the CSDL-designed flex pivot tester[20] on the as-polished surfaces. A disc-on-disc format for wear testing was initially examined and quickly discarded when extensive cocking problems were encountered. Pin-on-disc experiments were subsequently attempted using both TiB_2-composite and sapphire pins with different radii of curvature. Problems were encountered with the composite pin because it was flat. A curvature was subsequently placed on the edge of the composite pin. Wear tests with the sapphire pins always resulted in crayoning of the sapphire on the composite surface giving rise to a build-up of material as indicated by a surface profilometer.

Tests were additionally performed on the +30-μm and -10-μm specimens to see the effect of ceramic particle size on the wear and friction behavior of the material. The tests were conducted with sapphire, diamond, and TiB_2-composite pins contacting the selected 0.75-inch-diameter, roughly 0.25-inch-thick disk composite specimen. The composite disc was rotated at 100 r/min and friction traces obtained using a strip chart recorder. The values of the friction coefficients were calculated for these specimens at time intervals of 0.1, 1.0, and 10.0 minutes, which were measured from the start of the test. Friction traces were obtained at different applied loads. These were allowed to vary from 22 to about 300 grams.

No appreciable wear dependence of either composite on applied load was achieved. The data were fairly well behaved for wear runs versus a diamond stylus serving as the pin. The slight drop in the already low value of the friction coefficient with increasing time for most of the runs was interpreted as either resulting from the removal of an existing contaminating film on the surface or, more likely, from a polishing action on rough surface irregularities that were initially present. In any event, the data showed that the two composites could not be differentiated for wear resistance potential using this

procedure. In fact, both composites showed a superior wear resisting ability at loads which were much higher than would be encountered in an actual gas bearing. The data obtained with sapphire and composite pins resulted in substantially increased values of the friction coefficient which showed a significant rise with increasing time for both composites.

The implication of the above results was that composite parts should not be permitted to mate with parts of similar material in a wear circumstance such as what exists in a gas bearing. In lieu of diamond surfaces, with which good behavior was observed, experiments reported in Section 4 of this report indicated that this material possibly would be quite compatible with boron implanted surfaces. Results using diamond pins suggested that, as with the CVD-boron surfaces, the preparation of diamond-like surfaces on beryllium should be investigated for gas bearing application. The compatibility of the CVD and TiB_2-composite surfaces with the recently reported diamond-like films[27] might well prove adequate for application. In the preparation of such films, however, care would need to be exercised to prevent formation of beryllium-carbide, which is known to be susceptible to attack from moisture.

5.3.4 Production of Near-Net Shape Parts

Because of the many difficulties that are encountered in the machining of these materials using conventional procedures, it is important to be able to fabricate parts of this composite in near-net shape and size. The design that was examined was that of a cylindrical geometry with a hole running across the axis, as this forms part of a spool-type gas bearing.

Initial experiments dealt with hot isostatically pressing the required blend of powders (TiB_2 and beryllium) around a pre-machined 430 stainless steel mandrel shaped in the form of several ribbed sections to yield several parts in close-to-finished size. The 430 stainless was selected primarily because of its greater thermal expansion match to

beryllium and because it does not undergo a structural (and associated discontinuous dimensional) change at about 760°C.

The disadvantage in the use of this material, however, was that unlike low carbon steel, which is readily dissolved in a warm 50-percent solution of nitric acid, the 430 stainless needed to be machined. Because machining added substantial cost to the production of the part, low carbon 1020 steel was investigated (and used) during subsequent experimentation. Even though this resulted in reducing machining costs, primarily because it was easier to machine 1020 compared to 430 stainless, the machining costs were not eliminated entirely. The parts produced using 1020 steel, however, had high integrity and were found to be similar in quality to those produced earlier.

In addition to minimizing costs associated with machining of the composite and the steel, the production of parts which have a thermal expansion characteristic closely matched to beryllium is a very desirable objective. Measurements showed that thermal expansion coefficient values of these composites were on the order of about $5.0 \times 10^{-6}/°F$ compared to beryllium, whose expansion coefficient is about $6.4 \times 10^{-6}/°F$. To maximize the expansion behavior of the gas bearing part so as to more closely match that of beryllium, an alternative approach was selected. This consisted of fabricating the part essentially out of beryllium with no more than a 0.005- to 0.01-inch region of the surfaces (that are subjected to rubbing action) consisting of the composition of the composite. This was expected to assure a high expansion coefficient (extremely close to beryllium) for the fabricated part as well as result in parts that could be produced with less severe machining constraints.

A high quality metallurgical bond was formed between the base beryllium part and the composite layer that was bonded onto the beryllium structure. The composite was packed in the form of a powder blend of beryllium and TiB_2 particles at those surfaces of the machined beryllium which are subjected to rubbing action during operation of the

gas bearing. The (solid beryllium)-(composite powder) structure was HIPed together at 1050°C for two hours under an Argon pressure of 30 kpsi to promote densification and bonding of the powder to the beryllium structure. Figure 17 shows the high quality of the bond that was formed using this procedure. The fine structure observed within the beryllium was believed to be associated with the presence of very fine BeO particles dispersed at the grain boundaries of the instrument grade, I-400 beryllium that was selected to form the part. (I-400 beryllium has, typically, well over four weight percent BeO.) The purer quality of beryllium powder that was used to form the composite was evident in the much cleaner beryllium matrix that was found to exist in the region of the densified composite.

Mixed results were obtained in the parts that were produced, indicating the need for additional experimentation to further develop this procedure. Of the three parts that were produced using these procedures, only one appeared to be of acceptable quality after removal from the individual HIP cans. Upon subjecting this third part to finish grinding and lapping operations for producing hardware of acceptable quality, a small portion of the surface, which was in the neighborhood of the inner diameter of the cylindrical part, showed an inordinate amount of void content. This is shown in Figure 18. These observations suggested that perhaps the HIP operation should have been performed at still higher temperatures. A tighter packing of the blended composite powder about the required surfaces of the beryllium part would also have assisted in the production of higher quality material.

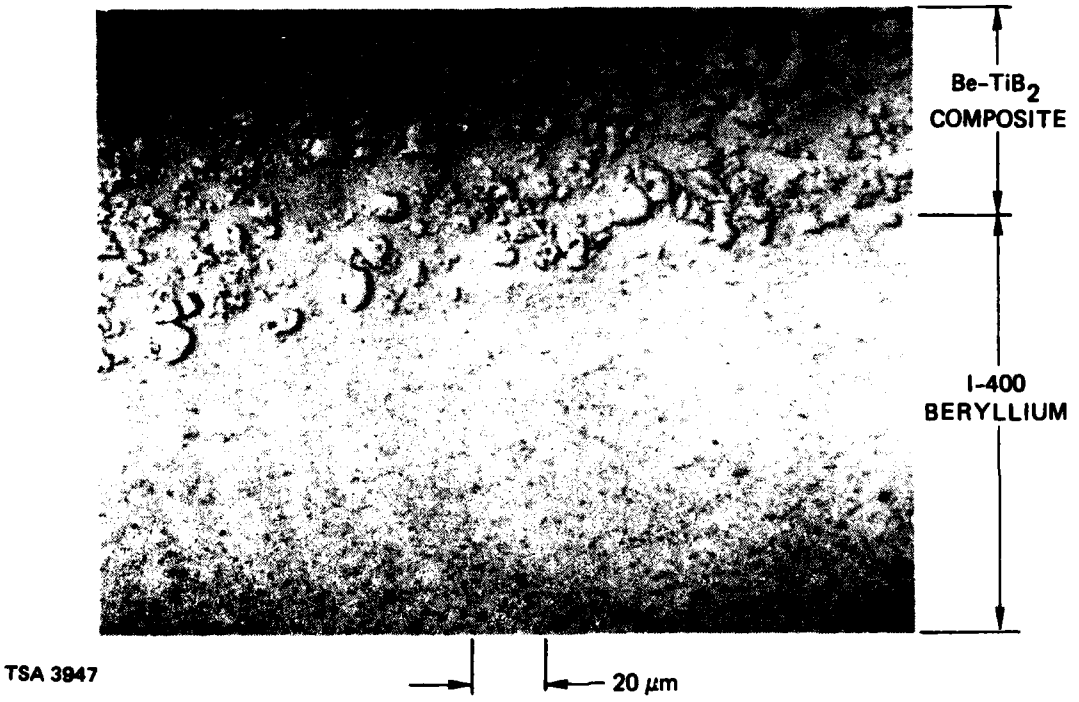

Figure 17. High quality bond formed between the Be-TiB_2 composite and the I-400 beryllium part.

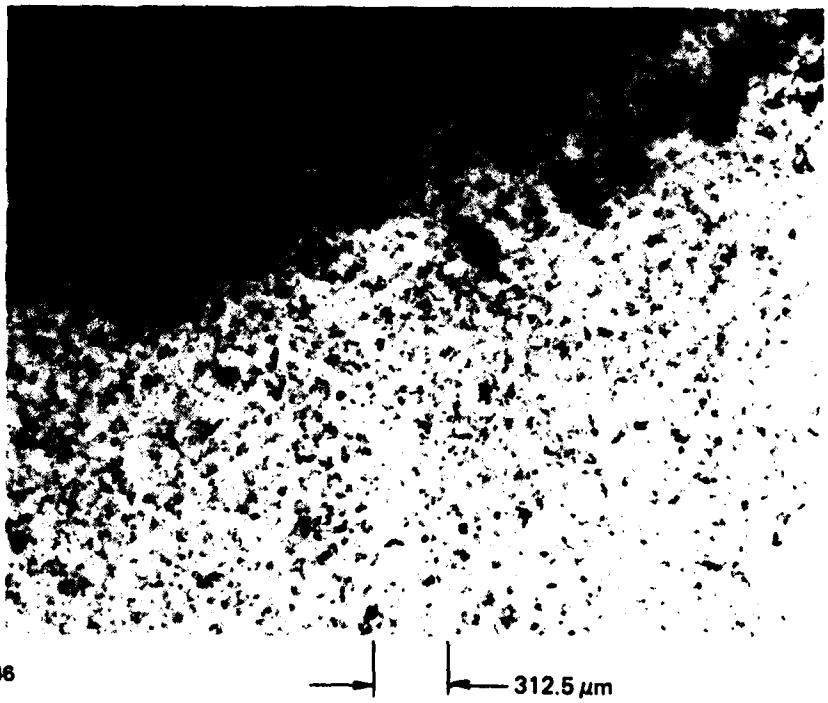

Figure 18. High void content observed in composite layer near the inner diameter of the coated-Be part.

SECTION 6

SUMMARY OF SIGNIFICANT FINDINGS

Research performed under this task was particularly rewarding. Of the three areas investigated, (1) CVD boron surfaces, (2) boron implanted surfaces, and (3) Be-TiB_2 composite, the latter two showed particular promise and were transitioned to hardware activities. Several of the significant findings from this effort are briefly noted below.

(1) Of the two gas systems investigated, BCl_3 reaction with hydrogen and thermal decomposition of B_2H_6, the latter was found to be the superior process for forming CVD boron films on beryllium at low (700 to 800°C) deposition temperatures.

(2) The quality of the CVD-boron deposited surface deteriorated when depositions were performed at high substrate temperatures (>900°C) and higher diborane gas concentrations. Uniformity of film thickness was achieved by the axial rotation of flat disk specimens.

(3) Even though CVD-boron surfaces showed extremely high values of microhardness (typically exceeding 2000 KHN), these surfaces were not found to be compatible with most surfaces, except diamond, which they were brought into contact with in a wear circumstance.

(4) The feasibility of implanting boron into beryllium at concentration levels of well over 50 atom percent was demonstrated. Instead of significant sputter erosion of the beryllium surface during implantion, build-up of material was observed to the extent expected from the added (implanted) species.

(5) Boron implantation resulted in substantial increases in hardness over that measured for unimplanted beryllium. Measurements indicated that heat treatment led to additional hardness increases. The implanted (and heat treated) surfaces were found to possess low friction and extremely good wear resistance properties versus potential (gas bearing) mating materials.

(6) Of the several implantation profiles (flat and graded) that were investigated for different peak, intended boron concentrations, samples with 40 atom percent boron appeared the best. Microhardness measurements were not found to provide sufficient information on the wear-resisting ability of the implanted surfaces. AES and RBS techniques were determined to be suitable for determining depth composition profiles of the implanted specimens.

(7) A new procedure was devised for reliably measuring the microhardness of these (CVD as well as boron-implanted) films. This consisted of making hardness measurements with a series of applied loads and extrapolating the data to low applied load values. A novel procedure was also devised for measuring the relative wear resisting ability of the implanted surfaces. This involved performing the wear tests at increasing values of the applied load and determining the load that resulted in catastrophic destruction of the surface.

(8) Gas bearing hardware produced using boron-implanted thrust plates, in a spool geometry, adequately demonstrated the suitability of these surfaces to gas bearing application. Repeated start-stop testing showed that these surfaces were quite resistant to wear at levels that were deemed acceptable for hardware purposes.

(9) Of the different ceramics investigated, TiB_2 was found best suited to forming a metal matrix composite with beryllium. The composite was fabricated from Be and TiB_2 powder blends using the HIP technique, which was developed for producing high integrity composites.

(10) Lapping studies showed that good, clean surfaces could be achieved on the coarse TiB_2 ceramic particles by appropriately developed procedures. Production-oriented techniques using diamond compounds resulted in extensive damage to the TiB_2 particles. The induced damage led to continuous particulate generation during cleaning of the part using ultrasonic means. Techniques were developed which were both oriented to production as well as capable of producing ceramic particle surfaces with minimal damage.

(11) Wear tests performed with the Be-TiB_2 composite samples showed that they were generally compatible with other materials of interest, in particular the boron-implanted beryllium surface.

(12) Techniques were developed for producing near-net shape hardware parts to minimize production costs related to grinding and machining processes. The near-net shape part, which was produced with partial success, was a cylinder with a hole running centrally down its axis. Efforts were additionally made at producing near-net shape parts which, in the main, consisted of beryllium and contained a thin layer of Be-TiB_2 composite (metallurgically bonded to the beryllium part) at the rubbing surfaces.

SECTION 7

RECOMMENDATIONS FOR FUTURE WORK

Based on the work performed under this program, the following are recommended for future work.

(1) Investigate the feasiblilty of producing diamond-like films on beryllium (without the formation of beryllium-carbide, which can be attacked by moisture). All three surfaces produced in this program have shown excellent tribological compatiblity with respect to a diamond pin in a pin-on-disc wear test.

(2) Further investigate surfaces produced by implantation of additional species such as nitrogen. The aim would be to study the effects on the wear resisting ability of the surface in comparison to what was observed for the binary Be-B system.

(3) Additionally evaluate implanted and heat treated boron-implanted beryllium surfaces to study the kinetics of the changes in boron distribution (and their accompanying wear resisting abilty) at the operating temperature, over the predicted life time(s) of the instruments(s).

(4) Develop near-net shape technology for economically producing production parts consisting wholly of the Be-TiB_2 composite material, or limiting the composite composition to the regions that see rubbing (in the part predominantly composed of beryllium).

REFERENCES

1. Rutherford, J.L., and W.B. Swain, Alumina Bearing in Gas-Lubricated Gyros, AIAA/ASME 8th Structural Dynamics and Materials Conference, California, NASA Report No. NASA-CR-88597, 29-31 March 1967.

2. Palmieri, J.R., Materials Research for Advanced Inertial Instrumentation, Task 2: Gas Bearing Material Development By Surface Modification of Beryllium, Technical Report R-1199, The Charles Stark Draper Laboratory, Inc., September 1978.

3. Das, D., K. Kumar, E. Wettstein, J. Wollam, Materials Research for Advanced Inertial Instruments, Task 2: Gas Bearing Material Development by Surface Modification of Beryllium, Technical Report R-1330, The Charles Stark Draper Laboratory, Inc., October 1979.

4. Das, D., K. Kumar, E. Wettstein, and J. Wollam, Materials Research for Advanced Inertial Instrumentation, Task 2: Gas Bearing Material Development, Technical Report R-1434, The Charles Stark Draper Laboratory, Inc., December 1980.

5. Das, D., K. Kumar, E. Wettstein, and J. Wollam, Materials Research for Advanced Inertial Instrumentation, Task 2: Gas Bearing Material Development, Technical Report R-1528, The Charles Stark Draper Laboratory, Inc., December 1981.

6. Das, D., and K. Kumar, Materials Research for Advanced Inertial Instrumentation, Task 2: Gas Bearing Material Development, Technical Report R-1647, The Charles Stark Draper Laboratory, Inc., December 1982.

7. McEwen, J., and R. Schluntz, History and Experience into Chromium Oxide (LC-4) Plasma Coating of Bearings by Union Carbide, Report No. C-4699, The Charles Stark Draper Laboratory, Inc., July 1976.

8. Advanced Inertial Technologies, Vol. III, Technical Report AFAL-TR-73-124, The Charles Stark Draper Laboratory, Inc., March 1974.

9. Kumar, K., Analysis of $W_{(x)}C$ Sputter Deposits, Report No. C-4749, The Charles Stark Draper Laboratory, Inc., December 1976.

10. Markovsky, L. Ya, D. Kondraskev Yu, and G.V. Kaputovskaya, "The Composition and Properties of Beryllium Borides," J. Gen. Chem. U.S.S.R., Vol. 25, 1955, p. 1007.

11. Hoenig, C.L., C.F. Cline, and D.E. Sands, "Investigation of the System Beryllium-Boron," J. Am. Ceram. Soc., Vol. 44, No. 8, August 1961, p. 385.

12. Laubengayer, A.W., D.T. Hurd, A.E. Newkirk, and J.L. Hoard, "Preparation and Properties of Pure Crystalline Boron," J. Am. Chem. Soc., Vol. 65, 1943, p. 1924.

13. Hoard, J.L., and A.E. Newkirk, "An Analysis of Polymorphism in Boron, etc.," J. Am. Chem. Soc., 82 (1960), p. 70.

14. Decker, B.F., and J.S. Kasper, "The Crystal Structure of a Simple Rhombohedral Form of Boron," Acta. Cryst., 12 (1959), p. 503.

15. Kumar, K., and D. Das, Differential Expansion Volume Compaction, US Patent No. 4,260,582, issued 7 April 1981.

16. Kumar, K., and D. Das, "Structure Modification of β-Boron by Plasma Spraying," Met. Trans., Vol. 11A, 1980, p. 1489.

17. Kumar, K., and D. Das, Method for Forming γ-Boron, U.S. Patent No. 4,342,734, issued 3 August 1982.

18. Das, D., and K. Kumar, "Chemical Vapor Deposition of Boron on Beryllium Surface", presented to International Conf. on Met. Coatings, San Francisco, April 1981, Thin Solid Films, 83, (1981), p. 53.

19. Das, D., and K. Kumar, "Tribological Behavior of Improved Chemically Vapor Deposited Boron on Beryllium," Thin Solid Films, 108, (1983), p. 181

20. Koehler, K., Flex Pivot Wear Tester--Design and Operation, Technical Report C-5413, The Charles Stark Draper Laboratory, Inc., June 1981 (ONR Contract No. N00014-77-C-0388).

21. Kant, R.A., J.K. Hirvonen, and J.S. Wollam, "Surface Hardening of Gas Bearing Materials by Ion Implantation," Thin Solid Films, 63 (1979), p. 27.

22. Kant, R.A., W.W. Hu, H. Herman, J.S. Wollam, R. Vardiman, and R.U. MacCrone, "Mechanical Properties of Ion Implanted Materials," presented at the Materials Research Society Symposium on Surface Modification of Materials by Ion Implantation, Cambridge, MA, November 1979.

23. Kant, R.A., A.R. Knudson, and K. Kumar, "Mechanical and Microstructural Properties of Boron Implanted Beryllium," 1981 Annual Meeting of the Materials Research Society Symposia Proceedings, Metastable Materials Formation by Ion Implantation, Editors: S. T. Picraux and W. J. Choyke, North-Holland, 1982, p. 253.

24. Kumar, K., H. Newborn, and R. Kant, "Wear Behavior of Flat and Graded Profile Boron Implanted Beryllium," presented at the Annual Meeting of the Materials Research Society, Boston, MA, November 1983 (to be published in Symposia proceedings).

25. Kumar, K., D. Das, and K. Koehler, "Beryllium-Ceramic Composites Using HIP for Gas Bearings", presented to the Annual Meeting of the American Ceramic Society, Washington, DC, May 1981.

26. Kumar, K., and D. Das, "Ceramic-Beryllium Composites for Gas Bearings," Amer. Ceram. Soc. Bull., 62 (1983), p. 249.

27. Green, A.K., and V. Rehn, "Surface Analysis of Diamondlike Carbon Films," J. Vac. Sci. Technol. A1(4) (1983), p. 1877.

BASIC DISTRIBUTION LIST

Organization	Copies
Defense Documentation Center Cameron Station Alexandria, VA 22314	12
Office of Naval Research Department of the Navy 800 N. Quincy Street Arlington, VA 22217	
ATTN: Code 471	1
Code 102	1
Code 470	1
Commanding Officer Office of Naval Research Building 114, Section D 666 Summer Street Boston, MA 02210	1
Commanding Officer Office of Naval Research Branch Office 536 South Clark Street Chicago, IL 60605	1
Naval Research Laboratory Washington, DC 20375	
ATTN: Code 6000	1
Code 6100	1
Code 6300	1
Code 6400	1
Code 2627	1
Naval Air Propulsion Test Center Trenton, NJ 08628 ATTN: Library	1
Naval Construction Batallion Civil Engineering Laboratory Port Hueneme, CA 93043 ATTN: Materials Division	1
Naval Electronics Laboratory San Diego, CA 92152 ATTN: Electron Materials Science Division	1
Naval Missile Center Materials Consultant Code 3312-1 Point Mugu, CA 92041	1
Commanding Officer Naval Surface Weapons Center White Oak Laboratory Silver Spring, MD 20910 ATTN: Library	1
David W. Taylor Naval Ship Research and Development Center Materials Department Annapolis, MD 21402	1
Naval Undersea Center San Diego, CA 92132 ATTN: Library	1
Naval Underwater System Center Newport, RI 02840 ATTN: Library	1

BASIC DISTRIBUTION LIST (Continued)

Organization	Copies
Naval Air Development Center Code 302 Warminster, PA 18964 ATTN: Mr. F.S. Williams	1
Naval Air Systems Command Washington, DC 20360 ATTN: Codes 52031 52032	1
Naval Sea System Command Washington, DC 20362 ATTN: Code 035	1
Naval Facilities Engineering Command Alexandria, VA 22331 ATTN: Code 03	1
Scientific Advisor Commandant of the Marine Corps Washington, DC 20380 ATTN: Code AX	1
Naval Ship Engineering Center Department of the Navy Washington, DC 20360 ATTN: Code 6101	1
Army Research Office PO Box 12211 Triangle Park, NC 27709 ATTN: Metallurgy and Ceramics Program	1
Metals and Ceramics Division Oak Ridge National Laboratory PO Box X Oak Ridge, TN 37380	

Organization	Copies
Naval Weapons Center China Lake, CA 93555 ATTN: Library	1
Naval Postgraduate School Monterey, CA 93940 ATTN: Mechanical Engineering Department	1
NASA Headquarters Washington, DC 20546 ATTN: Code RRM	1
NASA (216) 433-400 Lewis Research Center 21000 Brookpark Road Cleveland, OH 44135 ATTN: Library	1
National Bureau of Standards Washington, DC 20234 ATTN: Metallurgy Division Inorganic Materials Division	1
Director Applied Physics Laboratory University of Washington 1013 Northeast Fortieth Street Seattle, WA 98105	1
Defense Metals and Ceramics Information Center Battelle Memorial Institute 505 King Avenue Columbus, OH 43201	1

BASIC DISTRIBUTION LIST (Continued)

Organization	Copies
Army Materials and Mechanics Research Center Watertown, MA 02172 ATTN: Research Programs Office	1
Air Force Office of Scientific Research Building 410 Bolling Air Force Base Washington, DC 20332 ATTN: Chemical Science Directorate	1
Electronics and Solid State Sciences Directorate	1
Library Building 50, Room 134 Lawrence Radiation Laboratory Berkeley, CA	1
Los Alamos Scientific Laboratory PO Box 1663 Los Alamos, NM 87544 ATTN: Report Librarian	1
Argonne National Laboratory Metallurgy Division PO Box 229 Lemont, IL 60439	1
Brookhaven National Laboratory Technical Information Division Upton, Long Island New York 11973 ATTN: Research Library	1
Office of Naval Research Branch Office 1030 East Green Street Pasadena, CA 91106	1

SUPPLEMENTARY DISTRIBUTION LIST

Organization	Copies
Jack Bouchard Northrop/PPD 100 Morse street Norwood, MA 02062	1
Howard Schulien Department 6209 Bendix Corporation Guidance Systems Divisions Teterboro, NJ 07608	1
Don Bates Honeywell, Inc. Aerospace Division 11350 US Highway 19 St. Petersburg, FL 33733	1
R. Baldwin Honeywell, Inc. Avionics Division 2600 Ridgway Parkway Minneapolis, MN 55413	1
Bus Brady 62-11B/1 Lockheed Missile and Space Co., Inc. PO Box 504 Sunnyvale, CA 94088	1
Dan Fromm MS 1A1 Delco Electronics 7929 South Howell Avenue Milwaukee, WI 53201	1
F. Mikoliet Autometics Division Rockwell Internatio 1 3370 Miraloma Avenue Anaheim, CA 92803	1
P. Jacobson Sperry Flight Systems PO Box 21111 Phoenix, AZ	1
John Hanks Dynamics Research Corporation 60 Concord Street Wilmington, MA 01887	1
D. Riley Systems Group, Minutemen TRW, Inc. PO Box 1310 San Bernardino, CA 92402	1
Professor Robert Ogilvie Department of Materials Science and Engineering Massachusetts Institute of Technology Cambridge, MA 02139	
Dr. Glen R. Buell (D. Starks) AFML/MBT Wright-Patterson Air Force Base Dayton, OH 45433	1
Major George Raroha AFAL/CC Wright-Patterson Air Force Base Dayton, OH 45433	1

SUPPLEMENTARY DISTRIBUTION LIST (Continued)

Organization	Copies	Organization	Copies
Joe Jordan Litton Guidance and Control Systems 5500 Canoga Avenue Woodland Hills, CA 91364	1	Lt. Col. Gaylord Green Capt. Ken Wernle BMO/ENNG Norton Air Force Base San Bernardino, CA 92409	1
Bob Delaney Singer-Kearfott Division 150 Totowa Road Wayne, NJ 07470	1	Dave Gold (SP-230) Rick Wilson (SP-23411) Andy Weber (SP-23411) Strategic Systems Project Office Department of the Navy Washington, DC 20390	1
Elmer Whitcomb Sperry Gyroscope Division Great Neck, NY 11020	1	Lt. Col. Larry Fehrenbacker HQ/AFSC Andrews AFB, MD	1
C. Hoenig J. Holt R. Landingham Lawrence Livermore Laboratory University of California at Berkeley Livermore, CA 94550	1	N. Stuart (MMIRME) ALC/Ogden Ogden Air Logistics Command Hill AFB Ogden, UT 84404	1
Capt. S. Craig Aerospace Guidance Metrology Center Newark AF Station Newark, OH 43055	1	Professor R.M. Latanision Massachusetts Institute of Technology 77 Massachusetts Avenue Room E19-702 Cambridge, MA 02139	1
W. Lane Hamilton Standard Windsor Locks, CT	1	Dr. Jeff Perkins Naval Postgraduate School Monterey, CA 93940	1
Dr. A.G. Evans Department Material Sciences and Engineering University of California Berkeley, CA 94720	1	Dr. R.P. Wei Lehigh University Solid Mechanics Bethlehem, PA 18015	1
Professor H. Herman State University of New York Meterial Sciences Division Stony Brook, NY 11794	1	Professor H.G.F. Wilsdorf University of Virginia Department of Materials Science Charlottesville, VA 22903	

SUPPLEMENTARY DISTRIBUTION LIST (Continued)

Organization	Copies
Professor J.P. Hirth Ohio State University Metallurgical Engineering Columbus, OH 43210	1
Professor Peter Gielisse University of Rhode Island Division of Engineering Research Kingston, RI 02881	1
Dr. R.W. Rice Code 6360 Naval Research Laboratory 4555 Overlook Avenue, S.W. Washington, DC 20375	1
Professor G.S. Ansell Rensselaer Polytechnic Institute Department of Metallurgical Engineering Troy, NY 12181	
Professor J.B. Cohen Northwestern Univeresity Department of Materials Sciences Evanston, IL 60201	1
Professor M. Cohen Massachusetts Institute of Technology Department of Metallurgy Cambridge, MA 02139	
Professor J.W. Morris, Jr. University of California College of Engineering Berkeley, CA 94720	1
Larry Pope Sandia National Laboratories Division 5833 Alburquerque, NM 81785	1
Professor David Trunbull Harvard University Division of Engineering and Applied Physics Cambridge, MA 02139	1
Dr. D.P.H. Hasselman Montana Energy and MHD Research and Development Institute PO Box 3809 Butte, MT 59701	1
Dr. L. Hench University of Florida Ceramics Division Gainesville, FL 32601	1
Dr. J. Ritter University of Massachusetts Department of Mechanical Engineering Amherst, MA 02001	1
Professor G. Sines University of California at Los Angeles Los Angeles, CA 90024	
Director Materials Sciences Defense Advanced Research Projects Agency 1400 Wilson Boulevard Arlington, VA 22209	1

SUPPLEMENTARY DISTRIBUTION LIST (Continued)

Organization	Copies	Organization	Copies
Professor O.D. Sherby Stanford University Materials Sciences Division Banford, CA 94300	1	Professor H. Conrad University of Kentucky Materials Department Lexington, KY 40506	1
Dr. E.A. Starke, Jr. Georgia Institute of Technology School of Chemical Engineering Atlanta, GA 30332	1		

END

FILMED

5-84

DTIC